NATIONAL ADVISORY COMMITTEE FOR AERONAUTICS

REPORT 1326

FLIGHT AND ANALYTICAL METHODS FOR DETERMINING THE COUPLED VIBRATION RESPONSE OF TANDEM HELICOPTERS

By JOHN E. YEATES, Jr., GEORGE W. BROOKS, and JOHN C. HOUBOLT

1957

For sale by the Superintendent of Documents, U. S. Government Printing Office, Washington 25, D. C. Yearly subscription, $10; foreign, $11.25; single copy price varies according to size - - - - - - - - - Price 35 cents

REPORT 1326

FLIGHT AND ANALYTICAL METHODS FOR DETERMINING THE COUPLED VIBRATION RESPONSE OF TANDEM HELICOPTERS

By JOHN E. YEATES, Jr., GEORGE W. BROOKS, and JOHN C. HOUBOLT

Langley Aeronautical Laboratory
Langley Field, Va.

National Advisory Committee for Aeronautics

Headquarters, 1512 H Street NW., Washington 25, D. C.

Created by Act of Congress approved March 3, 1915, for the supervision and direction of the scientific study of the problems of flight (U. S. Code, title 50, sec. 151). Its membership was increased from 12 to 15 by act approved March 2, 1929, and to 17 by act approved May 25, 1948. The members are appointed by the President and serve as such without compensation.

FOREWORD

Several years ago it became evident from the results of some exploratory studies by the NACA that the helicopter, vibrationwise, could no longer be thought of as a simple system composed of several unconnected spring mass systems. In reality, all the spring mass systems are interconnected and each influences the other. It became evident that interaction or coupling of the components is important and must be considered in any vibration study. Coupling is of particular importance for helicopters, of which the components (fuselage, blades, etc.) have natural frequencies near one of the harmonics of rotor speed that is a multiple of the number of blades. In actual practice helicopter fuselages very often do have natural frequencies near one of the harmonics of rotor speed.

As a result of the increasing importance of this problem, a flight and analytical investigation was undertaken concurrently to investigate the coupled response of a tandem helicopter. This type of helicopter was selected because preliminary study indicated that the results might have more immediate application than would be true for other types available for flight test work.

The results of this joint investigation are reported herein.

CONTENTS

REPORT 1326

FLIGHT AND ANALYTICAL METHODS FOR DETERMINING THE COUPLED VIBRATION RESPONSE OF TANDEM HELICOPTERS [1]

By John E. Yeates, Jr., George W. Brooks, and John C. Houbolt

CHAPTER I

FLIGHT MEASUREMENTS OF THE VIBRATIONS ENCOUNTERED BY A TANDEM HELICOPTER AND A METHOD FOR MEASURING THE COUPLED RESPONSE IN FLIGHT

By John E. Yeates, Jr.

SUMMARY

A discussion of flight-test and analysis methods for some selected helicopter vibration studies is presented. The use of a mechanical shaker in flight to determine the structural response is reported.

The analysis methods described are based on the determination of the power spectral density of the force and of the response due to the force through use of analog frequency-analysis techniques. Results obtained by these methods are presented to show the coupled response of a helicopter in flight for two different blade configurations. The flight results are compared with results of ground tests to show the presence of coupling in flight. Available theoretical calculations of the coupled structural frequencies are included to show how these approximations compare with flight data. Some of the limitations of these tests and suggestions for refinement of flight vibration testing are discussed.

In addition, natural-vibration measurements of some of the more important harmonics of rotor speed are presented for a range of speed and power conditions.

INTRODUCTION

As helicopters have become larger and more flexible, the magnitude of the vibrations associated with these machines has increased. Available information indicates that high vibration levels are attributable to many sources, the primary sources being aerodynamic loading of the rotor blades and resonance amplification of the structure.

Because of speed changes and periodic variation in the angle of attack encountered by the rotor blades, alternating air forces act on the blades once per revolution and at multiples of this frequency. In general, only those forces which have a frequency that is a multiple of the number of blades per rotor are transmitted to the structure in the vertical direction. The alternating forces which are transmitted are usually small in comparison to the weight, but if the frequency of the transmitted force is near the structural resonance frequency, then large amplification may occur. In some of the early designs, attempts were made to lower the vibration level by setting the natural frequencies of the helicopter components, such as the blades, fuselage, and engine, between the multiples of rotor speed. This approach to the problem was only partially successful. Some calculations indicated that coupling of rotor blade bending and fuselage bending might bring about structural resonance at frequencies where none was apparent from considerations of each component separately. It became apparent that the helicopter must be treated as a coupled system and that the effect of the interaction of the components (blades, fuselage, engine, etc.) is important. The problem is to design and calculate more accurately so that determination of the coupled response frequencies of the structure is possible before the prototype is built.

As a result of the increasing importance of this problem, a flight investigation of the vibrations encountered by a typical tandem helicopter has been undertaken at the Langley Aeronautical Laboratory. Concurrently a theoretical investigation (ch. II) was undertaken to determine the coupled natural frequencies of a helicopter whose physical characteristics are practically identical to those of the helicopter used for the flight tests. The purpose of the present investigation was to determine the importance of coupling and to find out which structural components are of primary importance in calculating resonances. The helicopter chosen for this investigation was known to have a high vibration level under certain conditions; any changes that were made to this vibration level by the test methods would be recognized.

The response of the helicopter structure to mechanical shaking was measured at the front rotor under actual flight conditions. In addition, some flight surveys were made for a range of speed and power conditions and the natural vibrations were recorded.

[1] Supersedes NACA Technical Note 3852 by John E. Yeates, Jr., 1956, and NACA Technical Note 3849 by George W. Brooks and John C. Houbolt, 1956.

EQUIPMENT AND INSTRUMENTATION

HELICOPTER

A typical tandem helicopter with three-blade rotors was used for the investigation. During the tests the helicopter was equipped with two sets of blades (metal and wood) having different mass and frequency characteristics. (See fig. I–1 for details.)

INSTRUMENTATION

Motions of the structure were measured by using MB vibration pickups (type 124). Three components of velocity (vertical, longitudinal, and transverse) were measured at the front rotor, the rear rotor, and directly under the pilot's seat (fig. I–2). There were two pickups on the engine, and one on the fuselage near the engine which measured the vertical velocity only. Time histories of the output of these velocity pickups were recorded by an oscillograph. The velocity-pickup—oscillograph combinations have response curves which are similar to that of figure I–3. Response corrections have been applied to all the data. To provide the in-flight excitation a mechanical shaker (force varies as frequency squared) was mounted on the front-rotor gear box to shake in a vertical direction only. A tachometer measured the frequency of the shaker.

The flight conditions (airspeed, pressure altitude, etc.) were obtained through use of standard NACA recording instruments synchronized with the oscillograph by means of a common timing circuit.

ANALYSIS EQUIPMENT

The frequency-analysis equipment consisted of a two-channel, variable-filter-width heterodyne harmonic analyzer and associated playback and recording equipment. This device provides a reading of the mean square of the signal passed by a tunable filter with a specified accuracy of $\pm\frac{1}{2}$ decibel. The absolute accuracy with which the center frequency of the filter is known is estimated to be within 2 cps. In this case the data were analyzed at 20 times normal tape speed and therefore the center frequency is known to within 0.1 cps. The effective band width of the filter used for the data analysis was about 0.30 cps.

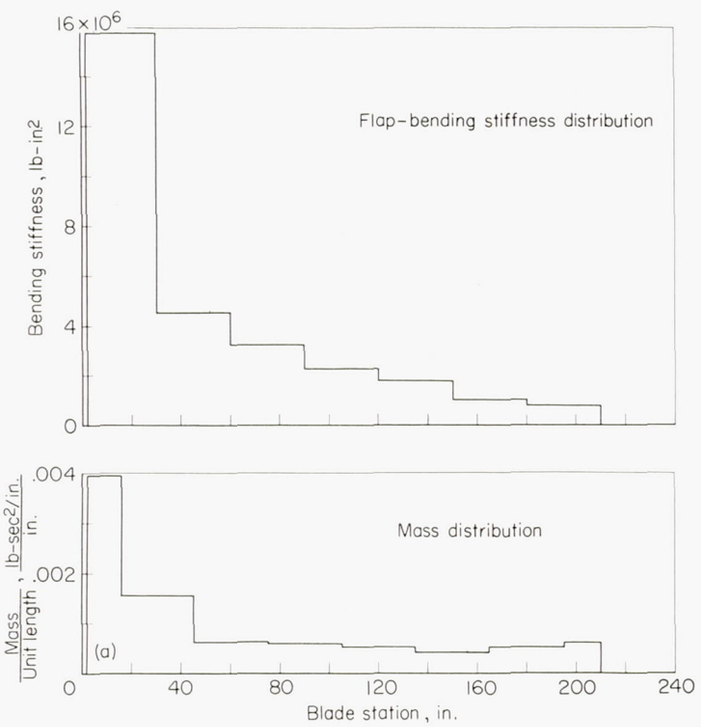

(a) Wood blades (natural frequency, 4.0 cps).

FIGURE I–1.—Mass and stiffness characteristics of the two sets of blades used for the tests.

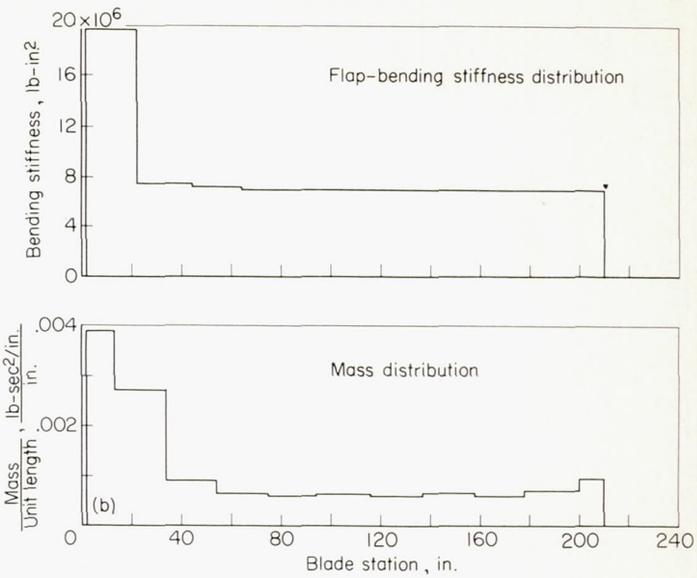

(b) Metal blades (natural frequency, 5.5 cps).

FIGURE I–1.—Concluded.

TESTS AND ANALYSIS METHODS

GROUND TESTS

Ground vibration tests were conducted with the same instrumentation as for the flight tests. The rotors (from the flapping pins out) were removed and the fuselage was suspended at the rotor hubs (fig. I–4) by soft springs (shock cord). The frequency of the fuselage as a whole on this spring suspension was less than 1 cps and would therefore have little effect on the elastic modes of the structure. The vibration response of the structure to excitation by a mechanical shaker was measured at the locations shown in figure I–1. The shaker, which was mounted on the front-rotor gear box, applied a sinusoidal force $F=0.45(\text{Frequency})^2$ in a vertical direction over the frequency range of 8 cps to 24 cps.

Since the natural frequency and effective mass of the rotors vary with rotor speed, only in flight are all the dynamic and aerodynamic characteristics of the helicopter correctly represented. In order to obtain some numbers for calculation purposes, the rotors were replaced by known weights and the change in fuselage response with change in weight was measured. The results of the measurements are shown in figure I–5. It can be seen that the first bending frequency of the fuselage, as indicated by the peaks, is decreased from 13.6 to 9.8 cps as the weight at each rotor is increased from 0 to 250 pounds.

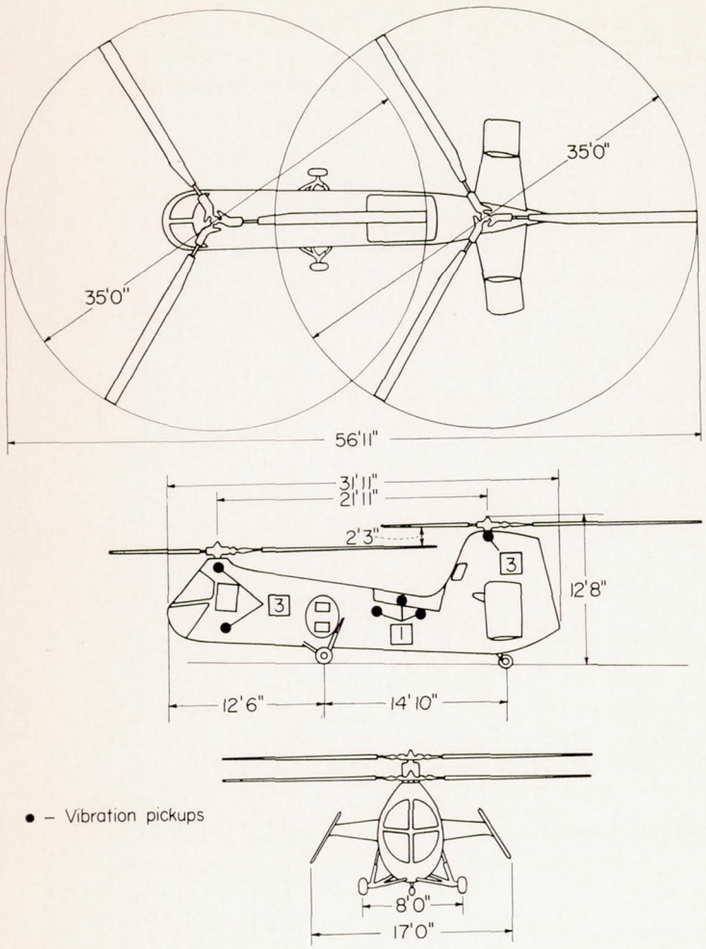

FIGURE I–2.—Test helicopter showing location of vibration pickups and number of components measured.

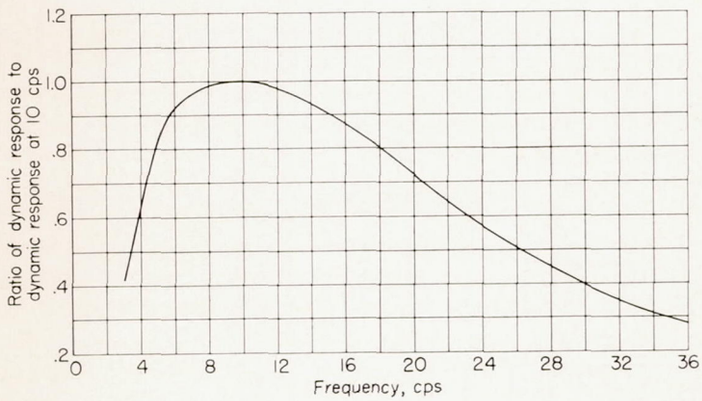

FIGURE I–3.—Typical response curve for vibration-pickup—oscillograph combination used.

FLIGHT TESTS

In a helicopter the natural vibrations are present to varying degrees for all flight conditions. Since the largest shaker available had a force output of about 75 pounds at the 3-per-revolution frequency (designated herein as 3-P) it was necessary to conduct the tests at flight conditions of minimum vibration. If the tests had been conducted at other flight conditions, the shaker force might have easily been overshadowed by the natural input, and the analysis would then

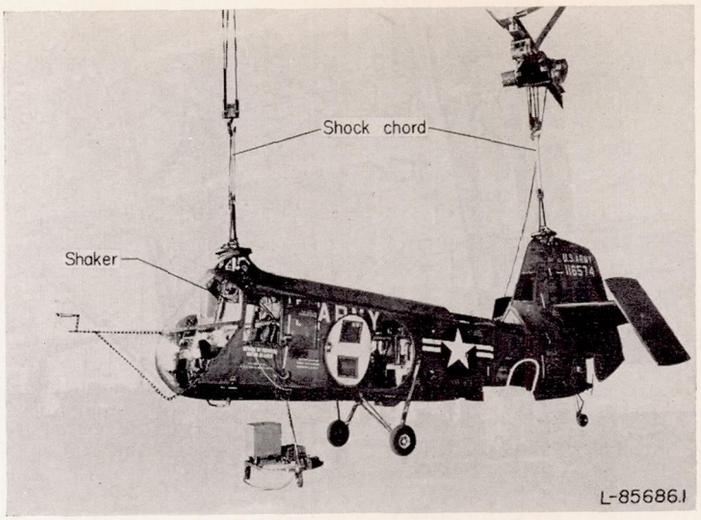

FIGURE I–4.—Test helicopter, with blade assemblies removed, showing method of suspension used for the ground vibration measurements.

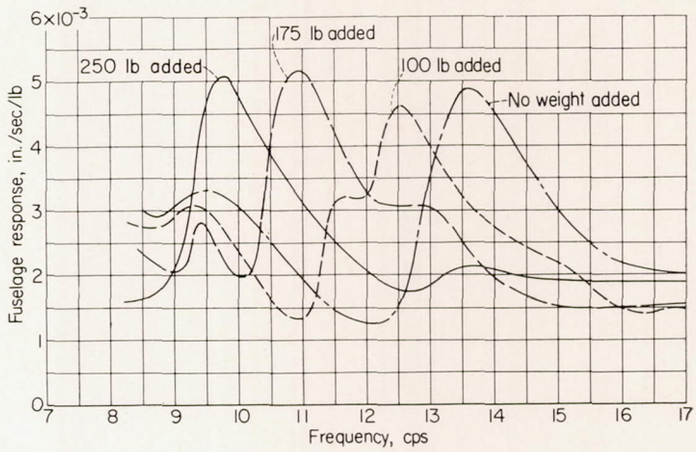

FIGURE I–5.—Variation of fuselage response measured at the front rotor with sinusoidal excitation applied at the front rotor (both blade assemblies replaced by weights from the flapping pin outward).

be very difficult if not impossible. In order to show the effect of changes in rotor speed, a series of rotor speeds was selected which encompassed the allowable range (250, 273, and 290 rpm). In the test helicopter the 3-P natural input occurs near a structural resonance frequency and structural vibrations are amplified. The vibrations in this frequency region are of most interest for several reasons—structural fatigue, pilot and passenger comfort, and so forth. The frequency of the shaker was therefore set to change slowly from 8 cps to 17.5 cps, the frequency range of interest. The sweep rate of the shaker was set at 6 seconds per cycle, which allowed approximately 1 minute for the traverse. The flight plan for the tests consisted of setting the power, airspeed, and rotor speed at predetermined values and holding them constant while the frequency of the shaker was varied from 8 cps to 17.5 cps. A similar run was made while the frequency of the shaker was varied in the reverse direction; thus two runs were made for each flight condition. Data were obtained for each of the three rotor speeds previously mentioned (250, 273, and 290 rpm). At 250 rpm the natural vibrations were so large that the additional

response due to the mechanical shaker could not be separated in the analysis. The results presented in this report are therefore for two rotor speeds only, 273 and 290 rpm.

The flight tests for the natural-vibration survey were conducted in a little different manner. The helicopter was trimmed for level flight at 45 knots and a desired power setting. The pilot then slowly traversed the range of speed above and below this trim speed, allowing as much as 3 minutes for the complete traverse. The rotor speed was set for 273 rpm and remained at this setting throughout the tests. Data were taken for four power conditions: take-off (37 in. Hg manifold press.), cruise (30 in. Hg manifold press.), low (20 in. Hg manifold press.), and autorotation (15 in. Hg manifold press.), over a speed range of approximately 15 to 90 knots.

ANALYSIS METHODS

In this helicopter the fuselage is considered to be similar to a free-free beam and the response of the structure is assumed to be the vertical motion of the front rotor resulting from the vertical force input of a mechanical shaker. Thus,

$$\text{Response}=\frac{\text{Output}}{\text{Shaker input}}$$

This relationship holds over the complete frequency range traversed by the shaker except for a small region near the 3–P frequency. The reason for this limitation is that the phase angle between the shaker force and the natural input force can have any value (0° to 360°) as the shaker sweeps through this 3–P frequency region, and these forces can either add or subtract.

Analog frequency-analysis techniques (ref. 1) were used for the data analysis. The sample records shown in figure I–6 were taken for flight conditions where the vibration was a minimum, a forward speed of 55 knots and a rotor speed of 290 rpm. The frequency of the shaker is indicated by a

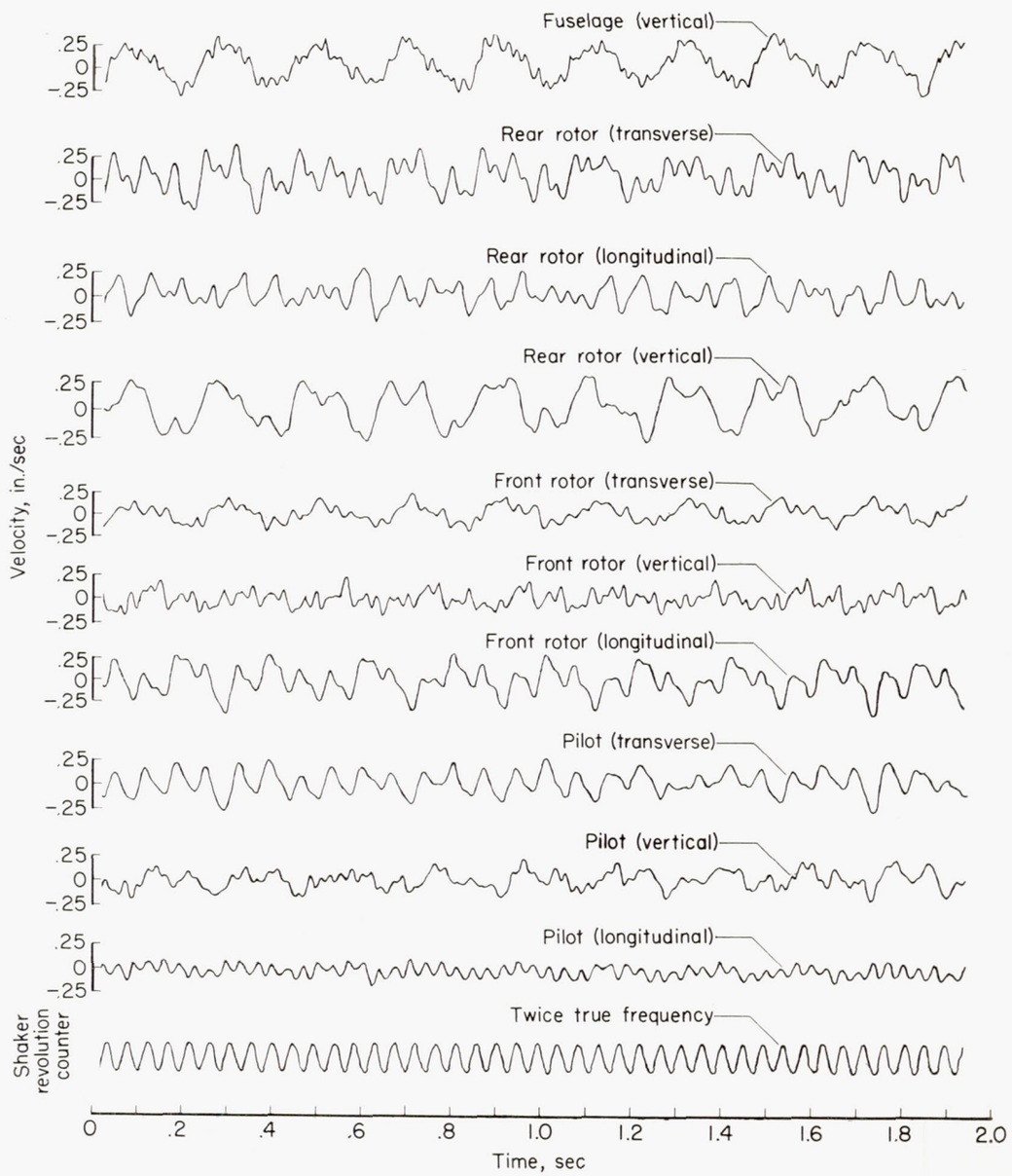

FIGURE I–6.—Typical record of some of the velocity components measured. Forward speed, 55 knots; rotor speed, 290 rpm; shaker operating.

revolution counter, the trace of which is shown in the lower part of the figure. Since the response measured at the front rotor in a vertical direction is considered representative of the structure, and because of the time required to work up the data, only this trace was analyzed.

The record was divided into four 15-second lengths for analysis to provide a larger ratio of signal to noise. The vertical velocity at the front rotor and the shaker force for each of the four sections of the records were transcribed manually from the original oscillograph record onto magnetic tape. The tape records were formed into loops and run through an electronic frequency analyzer. The output of the analyzer is in the form of a variation with frequency of the average square velocity or force passed by the filter as it sweeps through the frequency range. This output divided by the filter area provides an estimate of the power spectral density of the velocity and force time histories averaged over the length of the record, expressed as $\overline{(\text{in./sec})^2}$/cps and $\overline{\text{lb}^2}$/cps, respectively.

To illustrate the method for determining the coupled response of a helicopter in flight, figure I–7 is presented. The power spectral densities of the vertical velocity and shaker force at the front rotor are plotted against frequency for the four 15-second lengths of record, indicated by the numerals 1, 2, 3, and 4. During the first 15-second part of the record the helicopter responds to the shaker, as indicated by the velocity at the front rotor, in the frequency band swept by the shaker (8.5 to 11.6 cps). Since the natural vibrations are always present, a measurement of the first, third, and sixth harmonic inputs is also obtained. During the second 15 seconds of the record, the shaker sweeps from 11.6 to 13.9 cps and the output spectrum shows the helicopter responding in this frequency band and also provides a second measurement of the natural vibrations. It will be noted that, during the third 15-second portion of the record, the output due to the shaker and that due to the natural input are vectorially additive and no estimate of response to the 3–P frequency is obtained. In the fourth part of the record the helicopter responds in the frequency band swept by the shaker (15.9 to 17.6 cps) and an additional measurement of the natural vibrations is supplied. By breaking the record into four parts, it was possible to obtain three measurements of the 3–P component and four measurements of the 1–P and 6–P components without taking a separate record with the shaker not operating.

An indication of the variation of the natural input during the 1-minute record can be seen in the change in levels of the 1–P and 6–P components. There appears to be about ± 15 percent variation in the components over the total length of the record. With the information from figure I–7, the coupled response of the helicopter can now be determined. The total velocity-output spectrum (fig. I–7(a)) is divided by the shaker force spectrum (fig. I–7(b)) point by point, except in a small region near the 3–P frequency for reasons already explained in this section. The resulting curve is shown in figure I–8(b) and is a faired line through all the data points. In the small frequency band near the 3–P frequency, indicated by the hatched region in figure I–8(b), the response curve is unreliable. Data for the remaining response curves were handled in a similar manner.

RESULTS AND DISCUSSION

In order to show the effect of blade configuration and rotor speed, coupled-response curves for two types of blades (wood and metal) are presented for two rotor speeds. The flight-determined coupled-response frequencies are compared with those determined by the theory of chapter II for the wood blade configuration. Curves are also presented which show how the natural vibrations vary with forward speed for some selected flight conditions.

COUPLED RESPONSE WITH WOOD BLADES

In figure I–8 a comparison is shown of the coupled-response curves for 273 and 290 rpm. The two curves are similar, both having two peaks, but the relative heights of the peaks are different for the two rotor speeds. There appears to be an effect due to change in rotor speed; that is, when the rotor speed decreases, the height of the second peak decreases. It was concluded from the trend in the second peak for the two curves and from other data that there would be only one peak in the coupled-response curve for 250 rpm. It appears that at 250 rpm the natural input frequency and the fuselage coupled frequency would be so close together that large structural amplification would occur. This conclusion seems quite compatible with the fact that the records could not be unscrambled for this rotor speed.

COUPLED RESPONSE WITH METAL BLADES

In figure I–9 a comparison is shown of the coupled-response curves for 273 and 290 rpm. Here again the two curves are similar, both having two peaks, with the relative heights of the two peaks being different for the two rotor speeds. The effect of rotor speed is indicated by a reduction in height of the second peak as rotor speed decreases. The data through which these curves were faired had more scatter than those for the wood blades. Because the blade input is higher for the metal blades, the ratio of blade input to shaker force input is larger and it is harder to separate the responses in the frequency analysis. Near the 3–P frequency the separation of the response due to the shaker from that due to the natural input is very unreliable, as indicated in figure I–9.

The fact that the minimum level for the wood blades is lower than the minimum level for the metal blades near 13.5 cps evidences a possible change in the coupling of the helicopter components (blades, fuselage, etc.).

COMPARISON BETWEEN FLIGHT AND GROUND TESTS

In figure I–10 is shown a comparison of one of the flight response curves (273 rpm, wood blades) with the ground response curve for 100 pounds (45 percent flapping weight) at each rotor. The ground response curve for 100 pounds at each rotor was selected because the effective mass of each rotor was calculated to be 100 pounds in the first bending mode. Both the flight and ground measurements of vertical motion were taken at the front rotor. The comparison shows the presence of coupling. The ground response curve has one peak, whereas the flight response curves have two peaks in the frequency region of interest (10 to 16 cps).

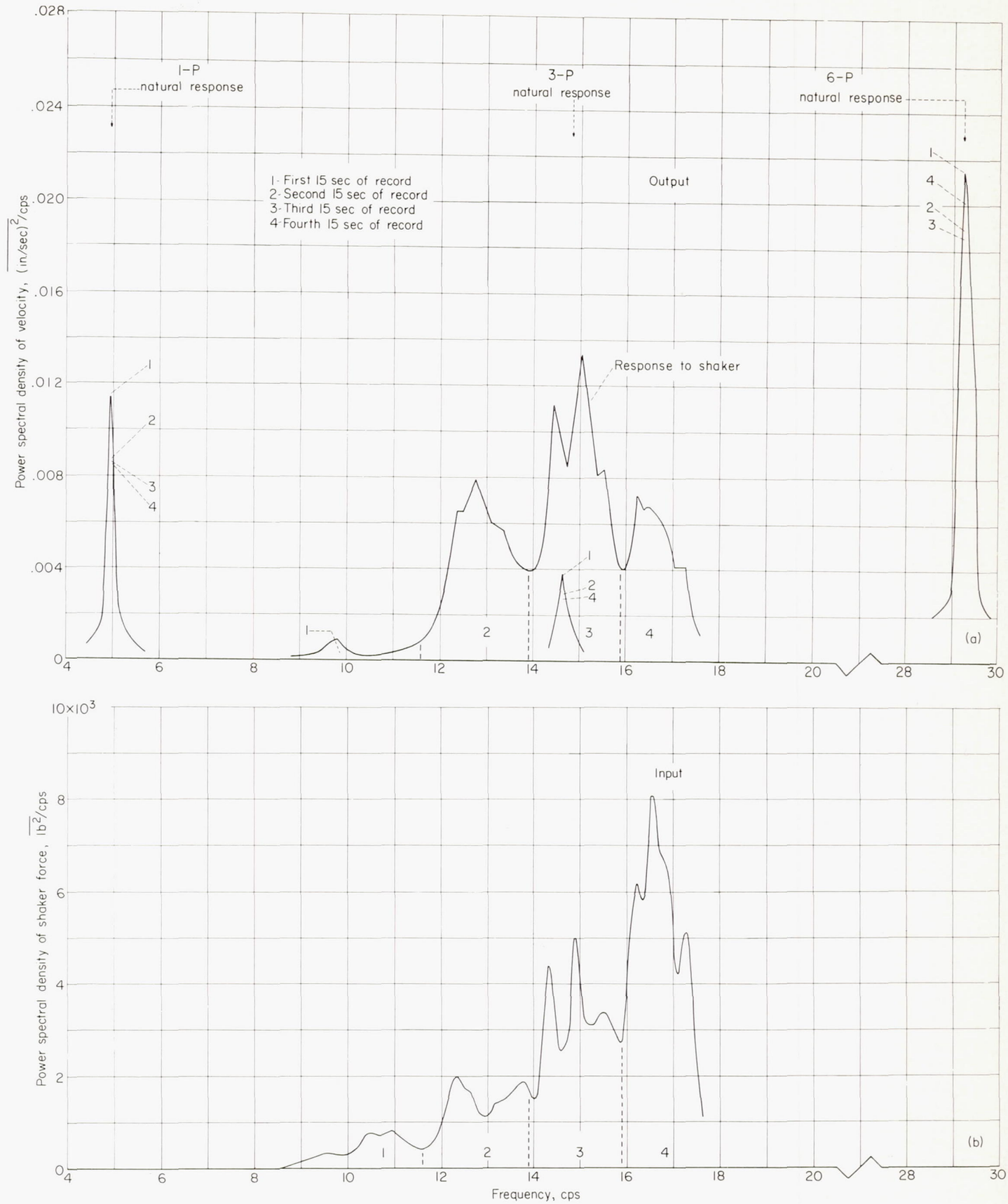

(a) Power spectrum of velocity at the front rotor.
(b) Power spectrum of shaker force at the front rotor.

FIGURE I–7.—Power spectra of the force and velocity at the front rotor with the shaker operating. Forward speed, 55 knots; rotor speed, 290 rpm: wood blade configuration.

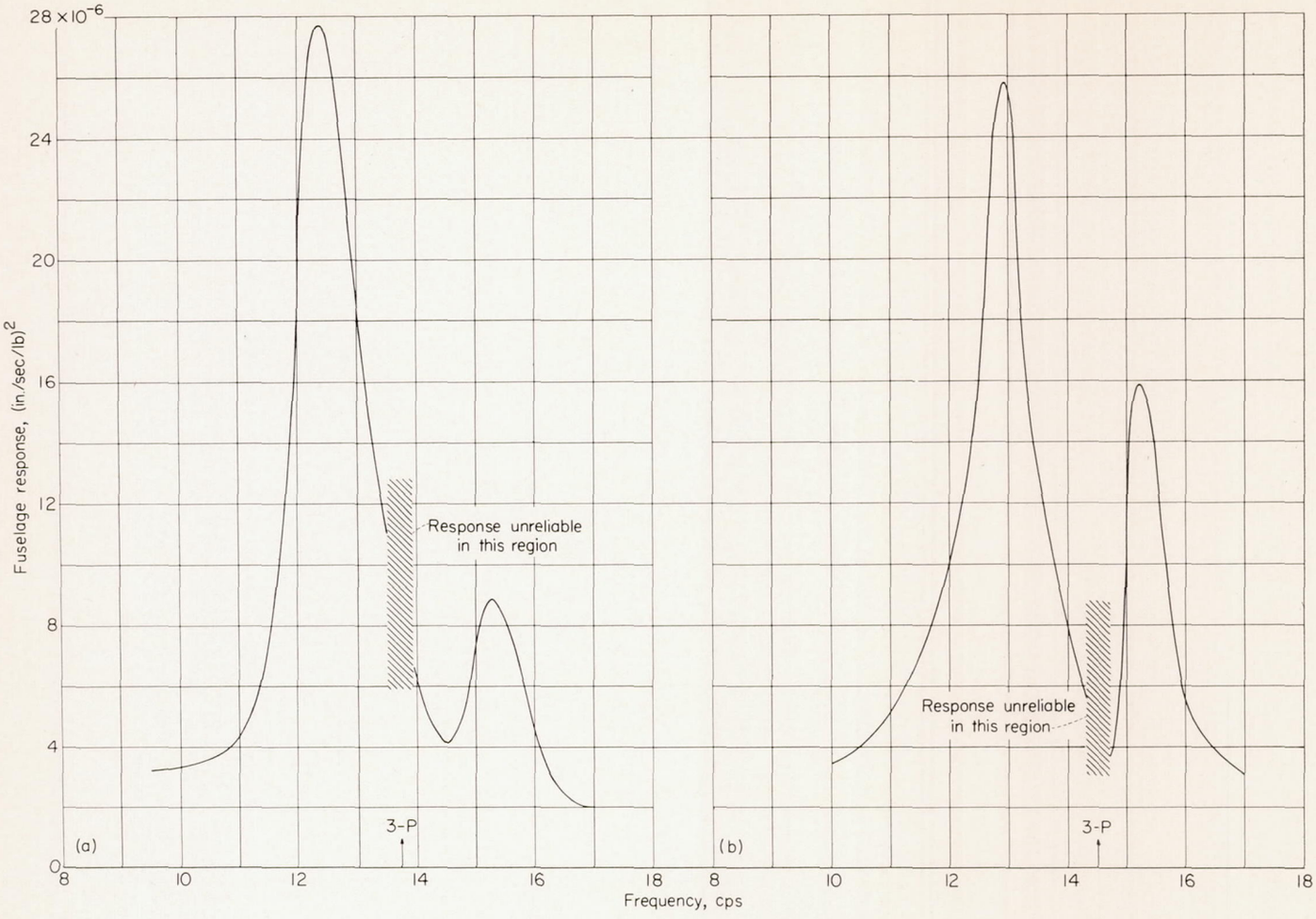

(a) 273 rpm. (b) 290 rpm.

FIGURE I–8.—*Coupled response of helicopter structure, measured at the front rotor, showing the effect of change in rotor speed for the wood blade configuration at a forward speed of 55 knots.*

COMPARISON OF FLIGHT RESULTS WITH THEORY

Since flight results are sometimes the only means for checking theoretical calculations, figure I–11 is presented to show a comparison between flight measurements and calculations by the theory of chapter II. The calculations, which were made by using blade parameters that correspond to those of the wood blades of this report, predict three modes of motion in the frequency range from about 12 to 15 cps. From an examination of several raw flight records, it was concluded that the two flight-measured structural modes are predominantly symmetrical. It was not possible to tell from the vibration records whether the predicted antisymmetric mode was present. However, since this antisymmetric mode is not one involving fuselage resonance, the fuselage acts primarily as a mass and very large blade motions are needed to produce any effect on the fuselage. On this basis it is not surprising that the antisymmetric mode would not be excited enough in flight to be measurable. The agreement between flight results and theory leaves room for improvement, but it does show how approximations for design purposes can be made.

SUGGESTIONS FOR REFINED FLIGHT-TEST TECHNIQUE

During the workup of the data some difficulties were encountered which were the result of flight-test techniques. Some suggestions for refinement in flight-testing techniques and some of the difficulties encountered are discussed in the following paragraphs.

Mechanical shakers were found to be very sensitive to speed control when exciting multidegree-of-freedom systems such as a helicopter. For the shaker used in the present investigation, the size and type of the drive motor was such that speed control was marginal. While cycling over a frequency range, the shaker tended to "lock in" whenever a resonance frequency was reached. This response of the shaker force to structural motion causes peaks in the average force input and motion output, frequency bands are skipped, and information is lost. In additon, the frequency is not known more precisely than to ± 0.1 cps and when the velocity spectrum is divided by the force spectrum, scatter is introduced in the coupled-response curves.

It was found from an examination of several runs for the same flight condition that the phase angle between the shaker force and the rotor force was different for each run. For this reason it was decided that a different flight-testing technique would be necessary for any future tests. The following flight-test technique is suggested for vibration response measurements. The forced excitation could be provided by a hydraulically actuated mass the frequency of which would be electronically controlled. With this type of

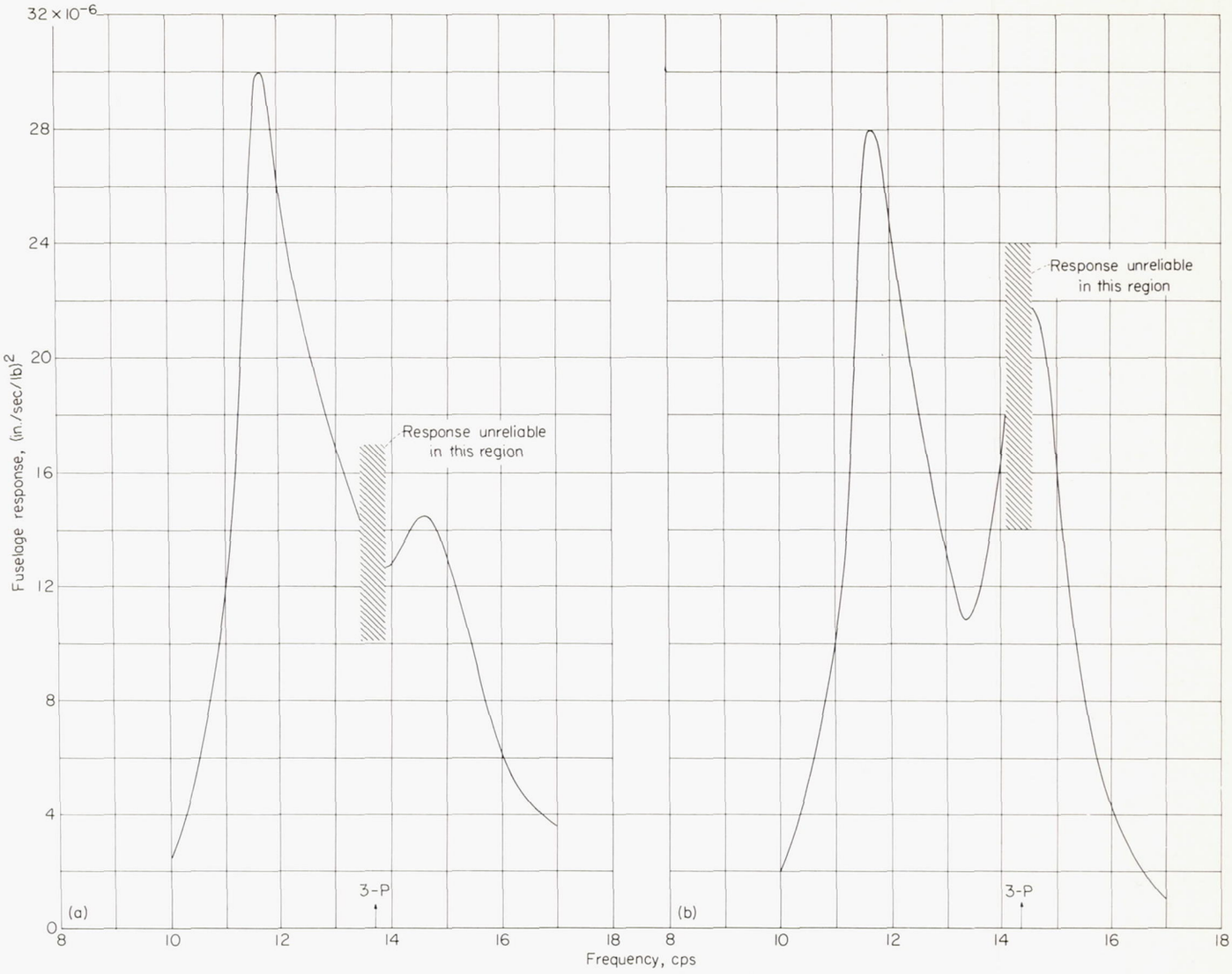

(a) 273 rpm. (b) 290 rpm.

FIGURE I–9.—Coupled response of helicopter structure, measured at the front rotor, showing the effect of change in rotor speed for the metal blade configuration at a forward speed of 55 knots.

shaker the amplitude of the force would be variable and, in addition, could be held constant over the frequency range. The same technique of sweeping would be used over most of the frequency range, except that within ±5 percent of any harmonic of rotor speed (1–P, 3–P, 6–P, etc.) a point-by-point approach would be used. In addition, the shaker would not be set on any frequency corresponding to a harmonic or rotor speed, since the phase between shaker input and structural output would be unknown, and the response at this frequency could not be determined. The response curve would be faired through these small regions near the harmonics of rotor frequency.

In the analysis the processing of the data could be greatly speeded up by recording the output of the vibration pickups directly on the tape, bypassing the transcriber. The data measurements could be handled more easily by using a flight tape recorder or by telemetering the information to the ground where it would be recorded on tape. This procedure would also allow the determination of the phase between the pickup locations.

NATURAL-VIBRATION MEASUREMENTS

The flight technique used for these measurements enabled the pilot to cover a range of speed for a minimum of flight time. Through the use of the previously mentioned frequency-analysis methods, it was possible to obtain time histories of some of the more important harmonics of rotor speed, such as the 3–P and 6–P components. For these time-history records, the filter was set at the component frequency (13.5 cps for 3–P and 27.0 cps for 6–P) and the entire length of tape was run through the analyzer. Figure I–12 will serve to illustrate a time history of one of the components, in this instance the 3–P. This is a 5-second sample record and is shown at 13.5 cps, the 3–P frequency. It can be seen that the 3–P component was not steady but varied somewhat in amplitude, even during this short record. This amplitude variation is apparently independent of airspeed.

In order to show the variation with airspeed of the harmonics of rotor speed, the 3–P and 6–P time-history records were read for 5-knot increments of airspeed, no attempt

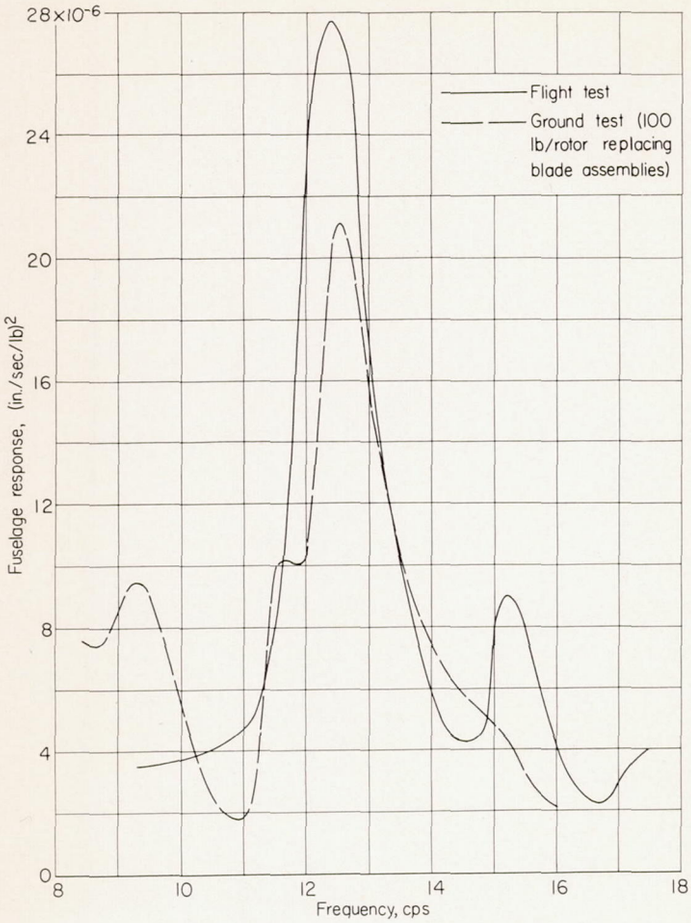

FIGURE I–10.—Coupled response of helicopter structure measured at the front rotor for wood blade configuration (rotor speed, 273 rpm; forward speed, 55 knots) compared with ground-measured response (100 pounds at each rotor replacing blade assemblies from the flapping pin outward).

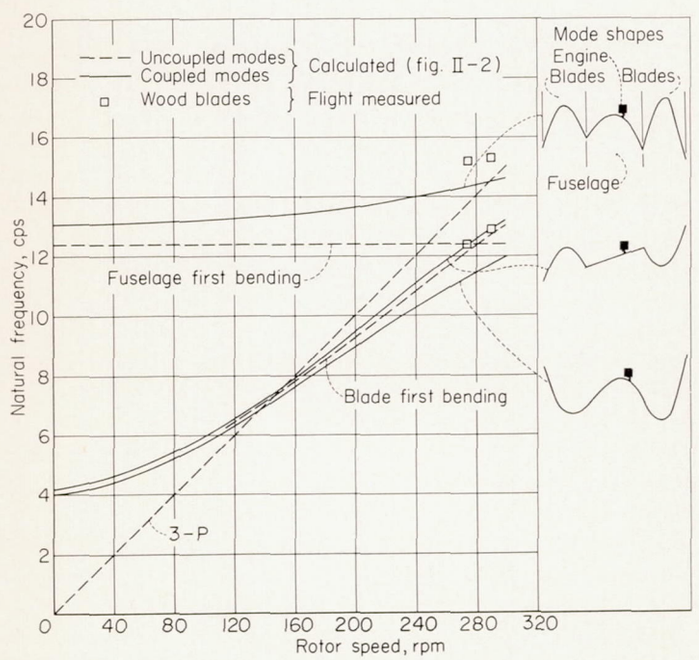

FIGURE I–11.—A comparison of flight-measured peak response frequencies with those determined by theoretical methods.

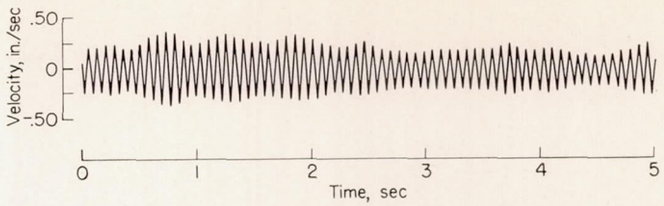

FIGURE I–12.—Sample record, showing the time variation of the 3–P component.

being made to average the variations in these components. The data points so obtained were converted to units of average displacement and are plotted against airspeed in figure I–13.

In figure I–13 the variation of the principal harmonics of rotor speed with airspeed are shown for four power conditions (take-off, 37 in. Hg; cruise, 30 in. Hg; low, 20 in. Hg; and autorotation, 15 in. Hg). All the natural-vibration data presented here were measured at the front rotor in a vertical direction and are for the metal blade configuration. In addition, all of the results shown in figure I–13 were obtained out of the ground-effect region. The scatter of the data points is indicated by the width of the bands in figure I–13. The 3–P component in this figure apparently is different for each power condition; however, two facts are evident: (a) in the low-speed range the higher the power setting, the higher the amplitude of vibration, and (b) the speed for minimum vibration is different for each power condition. In figure I–13 (b) the left portion of the 3–P curve was recorded on one day and the right portion on another, and the result illustrates how the records can vary from day to day.

For take-off and cruise power conditions the 6–P component shows its highest level of vibration near the low end of the speed range. The 6–P component for take-off power rapidly decreases to about 0.007 inch near 25 knots, and remains about constant over the remainder of the speed range. For cruise power the 6–P component slowly decreases to about 0.005 inch near 50 knots and remains near this amplitude over the remainder of the speed range. The 6–P component for the low and autorotation power conditions remains nearly constant over the speed range at about 0.006-inch amplitude.

It can be pointed out here that the relative magnitudes of the harmonic components change for different flight conditions. This variation could account for the fact that prototype changes which reduced vibration for one flight condition might be ineffective or adverse for another.

Measurements near transition in ground effect.—It was not possible to make a frequency analysis of the vibration measurements during transition because of trace overlap; therefore it was decided to analyze the records near transition to compare the output of all the vibration pickups. Transition is generally used to refer to a flight condition intermediate between hovering and the speed for minimum power, and is defined in this report as the speed region from 15 to 30 knots. Since flow asymmetries and associated vibrations tend to reach a peak in this region, the term is loosely used to refer to the speed where vibration first reaches a maximum. In table I–1 are given all the measured vibratory amplitudes (near transition) in terms of average displacement for each

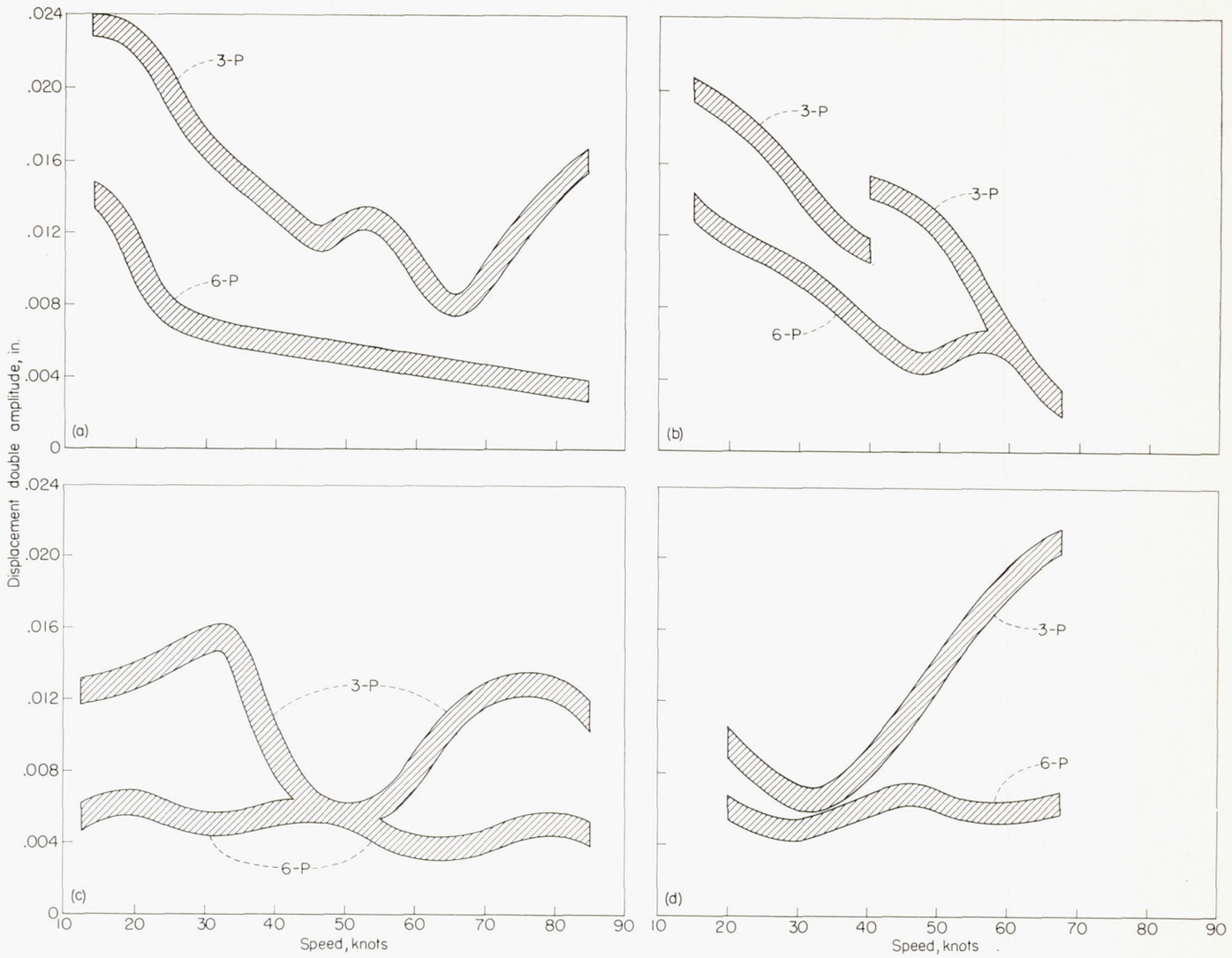

(a) Take-off power (37 in. Hg manifold press.).
(b) Cruise power (30 in. Hg manifold press.).
(c) Low power (20 in. Hg manifold press.).
(d) Autorotation (15 in. Hg manifold press.).

FIGURE I–13.—Variation of the principal harmonics of rotor speed with airspeed for four power conditions. Metal blade configuration.

TABLE I–1.—VIBRATION MEASUREMENTS MADE DURING APPROACH TO TRANSITION

Vibration-pickup location	Double amplitude of vibration, in., for—		
	1–P	3–P	6–P
Wood blades			
Pilot, longitudinal	0.0043	0.0016	0.0010
Pilot, vertical	.0090	.0103	.0027
Pilot, transverse	.0132	.0039	.0013
Front rotor, longitudinal	.0160	.0033	.0020
Front rotor, vertical	.0015	.0075	.0010
Front rotor, transverse	.0070	.0045	.0010
Rear rotor, vertical	0	.0061	.0020
Rear rotor, longitudinal	0	.0114	.0040
Engine, rear, vertical	0	.0141	0
Metal blades			
Pilot, longitudinal	0.0078	0.0054	0
Pilot, vertical	.0071	.0077	.0016
Pilot, transverse	.0170	.0088	0
Front rotor, longitudinal	.0120	.0117	0
Front rotor, vertical	.0074	.0094	.0020
Front rotor, transverse	.0074	.0053	0
Rear rotor, vertical	0	.0153	0
Rear rotor, longitudinal	.0230	.0362	0
Rear rotor, transverse	.0210	.0306	0
Engine, rear, vertical	0	.0125	0
Engine, forward, vertical	.0096	.0078	0
Fuselage, vertical	.0120	.0051	0

of the two blade (metal and wood) configurations. It can be seen in the table that the major vibrations are at the rear rotor, the longitudinal component being the largest. The raw flight records show that 4 seconds later, when the helicopter is experiencing transition conditions, the vertical component at the front rotor is the largest. From rough measurements of the raw records it is estimated that the vertical component at the front rotor (metal blades) has increased fivefold to about 0.05-inch double amplitude, whereas the components at the rear rotor have decreased markedly. In addition, it was concluded from an examination of the raw records (metal blades) for each of the two flight conditions previously mentioned that the fuselage mode of motion was primarily symmetrical. There is some evidence of the presence of an antisymmetric fuselage mode which could account for the change in the ratio of the vertical components of the front and rear rotors as the helicopter enters transition.

Estimate of force input at front rotor.—In order to define the magnitude of the force input at the front rotor and to illustrate how response curves of the type shown in figure I–8 can be used, the following example is presented: For

calculation purposes continue the response curve of figure I–9 (a) (273 rpm) through the hatched area; the response at the 3–P frequency in the hatched area of this figure is considered to be accurate within ±30 percent. By making use of the survey data of figure I–13, an estimate of the natural force input (metal blades) at the front rotor can be made for each of these power conditions over the speed range. For example, the response at the front rotor near the 3–P frequency is about 3.6×10^{-3} in./sec/lb (fig. I–9, 273 rpm) and the average displacement of the 3–P component for take-off power is 0.02-inch double amplitude near 25 knots (fig. I–13). Converting 0.02 inch at 3–P (13.7 cps) to velocity gives 0.86 in./sec; dividing this value by 3.6×10^{-3} in./sec/lb indicates about 240 pounds of vertical force input to the front rotor. This value of force is estimated to be correct within ±75 pounds. If survey records of the natural vibrations were available for the wood blade configuration, similar estimates of the force could also be made.

CONCLUDING REMARKS

A method is presented which enables the coupled structural response of a helicopter in flight to be determined. This method, which includes the use of a mechanical shaker for flight excitation, provides a great saving in flight and analysis time by using the technique of sweeping rather than a series of steady conditions. Results are presented which show the coupled response of a helicopter in flight for two different blade configurations. A modified flight-testing technique is suggested for future work. In addition, natural-vibration measurements of some of the more important harmonics of rotor speed are presented for a range of speed and power conditions.

The presence of the coupling of the components (fuselage, blades, etc.) is evidenced by the fact that the flight response curves show two peaks whereas the ground response curves show only one. The coupled-response curves for the two blade configurations (metal and wood) show the effect of change in rotor speed; that is, when the rotor speed is decreased the height of the second peak decreases.

A comparison of calculated coupled frequencies from available theory with those determined from flight tests indicates that the theory can give fair approximations to the coupled frequencies.

Numerical results on natural vibrations have been obtained and serve to confirm the expectation that significant variations in the relative harmonic contents of these natural vibrations occur with variations in flight conditions. The ability to make these measurements of the natural-vibration spectra should help in the evaluation of prototype helicopters and should point the way to changes for overall improvement.

REFERENCE

1. Smith, Francis B.: Analog Equipment for Processing Randomly Fluctuating Data. Aero. Eng. Rev., vol. 14, no. 5, May 1955, pp. 113–119.

CHAPTER II

ANALYTICAL DETERMINATION OF THE NATURAL COUPLED FREQUENCIES AND MODE SHAPES AND THE RESPONSE TO OSCILLATING FORCING FUNCTIONS OF TANDEM HELICOPTERS

By George W. Brooks and John C. Houbolt

SUMMARY

A method is presented for the analytical determination of the natural coupled frequencies and mode shapes of vibrations in the vertical plane of tandem helicopters. The coupled mode shapes and frequencies are then used to calculate the response of the helicopter to applied oscillating forces. Degrees of freedom included in the analysis are translation, pitching, and bending of the fuselage; translation, flapping, and bending of the blades; and translation of the engine. The method employs the Lagrange dynamical equations for free vibrations in conjunction with the kinetic and potential energies of the system in order to obtain the differential equations of motion for the coupled system which are then written in matrix form. The elements of the determinant of the matrix equation include the natural frequencies, mode shapes, and mass distributions of the uncoupled components of the helicopter (such as fuselage, blades, and engine) and permit the inclusion of experimental data of the uncoupled components in the evaluation of the coupled frequencies of the coupled system.

The results of calculations made for a particular tandem helicopter show the variation of the coupled frequencies with rotor speed and indicate the changes in the coupled frequencies which result from changes in the structural properties of the individual helicopter components. Calculated response curves show how the vibrations of the cockpit vary with the frequency and method of application of oscillating forces applied at the hubs. Suggestions for further refinement of the analysis to aid in the determination of the coupled frequencies for more complex and realistic systems are also presented.

INTRODUCTION

In many cases the development of the prototype of a particular helicopter is impeded because severe structural vibrations are encountered. Such vibrations often limit the utilization of production articles because of fatigue of the component parts of the structure as well as of the operating personnel. Available information indicates that the high levels of vibration are attributable primarily to two factors; namely, the high periodic content of the aerodynamic loading on the rotor blades and the amplification of the structural deformations due to proximity of resonance. Accordingly, it appears that the vibration levels may be reduced either by reducing the levels of the oscillating aerodynamic loads, by the inclusion of appropriate damping, or by choosing the natural frequencies of the coupled structure so that they are as far as possible from the integral multiples of the rotor speed.

The present report relates to resonance amplification and, in particular, to the determination of the natural frequencies, mode shapes, and response of the coupled helicopter structure as it exists in flight. Conventional methods such as those of references 1 and 2 may be used to predict the natural frequencies of the various components of helicopters such as fuselages, blades, and engines. Reference 3, which reports on the initial part of the present investigation, presents a method for the prediction of the natural frequencies and mode shapes of the structure which result when the various components are coupled together. The purpose of this analysis is to elaborate on reference 3 and to present a method for utilizing the resulting coupled frequencies and mode shapes in computing the response of the helicopter to applied oscillating loads.

The method is an energy method that involves chosen modes and frequencies of the uncoupled components which may be determined either by expressing the potential energy of the components in terms of given stiffness and mass distributions or, preferably, from experimental vibration tests of the components. The method is given in terms of a tandem-helicopter configuration but other configurations can be treated in an analogous manner.

The present report is concerned primarily with vibrations in the vertical plane—in particular, with fuselage translation, pitching, and bending; rotor-blade translation, flapping, and bending; and engine translation. The characteristic frequency determinant is derived, and calculated values for the natural coupled frequencies and mode shapes for a particular tandem helicopter are presented. These mode shapes and frequencies are then used to determine the vibration amplitudes of the cockpit which occur when oscillating forces are applied at the front and rear rotor hubs. The results of some trend studies are also presented to show the effect of variations of the uncoupled frequency of the fuselage and of the Southwell coefficient of the rotor blades on the coupled frequencies of the helicopter.

SYMBOLS

a_0, a_1	coefficients of front-rotor-blade modal deflections $\frac{r_F}{R_F}$ and x_1, respectively, in.
A_0, A_1, B_0, B_1 C_0, C_1, D_0, D_1	coefficients of frequency determinant (defined after eq. (11))
b_0, $\overline{b}_0$, b_1	coefficients of fuselage modal deflections 1, $\frac{s}{l}$, and y_1, respectively, in.
c_0, c_1	coefficients of rear-rotor-blade modal deflections $\frac{r_R}{R_R}$ and z_1, respectively, in.
EI	structural stiffness of helicopter at station σ, lb-in.^{2}
$(EI)_F$	structural stiffness of front rotor blades, lb-in.^{2}
$(EI)_R$	structural stiffness of rear rotor blades, lb-in.^{2}
$(EI)_f$	structural stiffness of fuselage, lb-in.^{2}
F	applied forcing function (see eq. (12)), lb
F_0	amplitude of applied forcing function
g_h	structural damping coefficient

k radius of gyration of mass of fuselage about front rotor hub, in.

K_e spring constant for engine mounts, lb/in.

$K_{F,1}$, $K_{R,1}$ Southwell coefficients for blade first elastic flapwise bending mode (defined after eq. (11))

l distance between front and rear rotors, in.

l_{cg} distance from front rotor hub to center of gravity of fuselage, in.

l_e distance from front rotor hub to engine, in.

L overall length of helicopter, in.

m mass per unit length of helicopter at station σ, lb-sec^2/in.^{2}

m_F mass per unit length of front rotor blade, lb-sec^2/in.^{2}

m_R mass per unit length of rear rotor blade, lb-sec^2/in.^{2}

m_f mass per unit length of fuselage, lb-sec^2/in.^{2}

M_F mass of front rotor blade, lb-sec^2/in.

M_R mass of rear rotor blade, lb-sec^2/in.

M_e mass of engine, lb-sec^2/in.

M_f mass of fuselage, lb-sec^2/in.

$M_{f,1}$ effective mass of fuselage (defined after eq. (11)), lb-sec^2/in.

M_r effective mass of helicopter in rth mode (see eq. (17)), lb-sec^2/in.

p, q number of blades on front and rear rotor, respectively

P_r, Q_r real and imaginary parts of response of helicopter in rth mode (see eqs. (23) and (24)), in.

r_F radial position of any blade element on front rotor (see fig. II–1), in.

r_R radial position of any blade element on rear rotor (see fig. II–1), in.

R_F radius of front rotor, in.

R_R radius of rear rotor, in.

s longitudinal position of any fuselage element (see fig. II–1), in.

t time, sec

T centrifugal force on blade at any radial station, lb; kinetic energy, lb-in.

T_F, T_R centrifugal force on front and rear rotor blades, respectively, lb

$\overline{T}_F$, $\overline{T}_R$ centrifugal force divided by square of rotor speed, lb-sec^2

V potential energy, lb-in.

w deflection of engine, in.

w_f deflection of engine with respect to fuselage, in.

x deflection of element of front rotor blade, in.

x_1 uncoupled first-bending-mode shape for front rotor blade

X, Y real and imaginary parts of response of helicopter (see eq. (26)), in.

y deflection of element of fuselage, in.

y_1 uncoupled first-bending-mode shape for fuselage

z deflection of element of rear rotor blade, in.

z_1 uncoupled first-bending-mode shape for rear rotor blade

α_r coefficient of deflection of rth coupled mode of helicopter (see eqs. (13) and (23)), in.

$\alpha_{r,0}$ amplitude of α_r, in.

σ distance measured rearward from leading edge of front rotor disk (see fig. II–1), in.

σ_A value of σ where oscillating force is applied

ϕ deflection of helicopter in response to applied force F (see eqs. (13) and (25)), in.

ϕ_r rth-coupled-mode shape of helicopter

$|\phi|$ amplitude of ϕ (see eq. (26)), in.

ω natural frequency of coupled modes; frequency of applied oscillating force, radians/sec

$\omega_{F,1}$, $\omega_{R,1}$ first natural uncoupled flapwise bending frequency of front and rear rotor blades, respectively, radians/sec

$\omega_{f,1}$ first natural uncoupled vertical bending frequency of fuselage, radians/sec

ω_e natural vertical frequency of engine on its mounts, radians/sec

ω_r natural frequency of rth coupled mode of helicopter, radians/sec

Ω rotor speed, radians/sec

The deflection in the first bending mode of the fuselage, measured at station s, is denoted by $y_1(s)$. For example, $y_1(0)$ is the deflection of the fuselage in first mode bending at the front rotor hub. (See fig. II–1.)

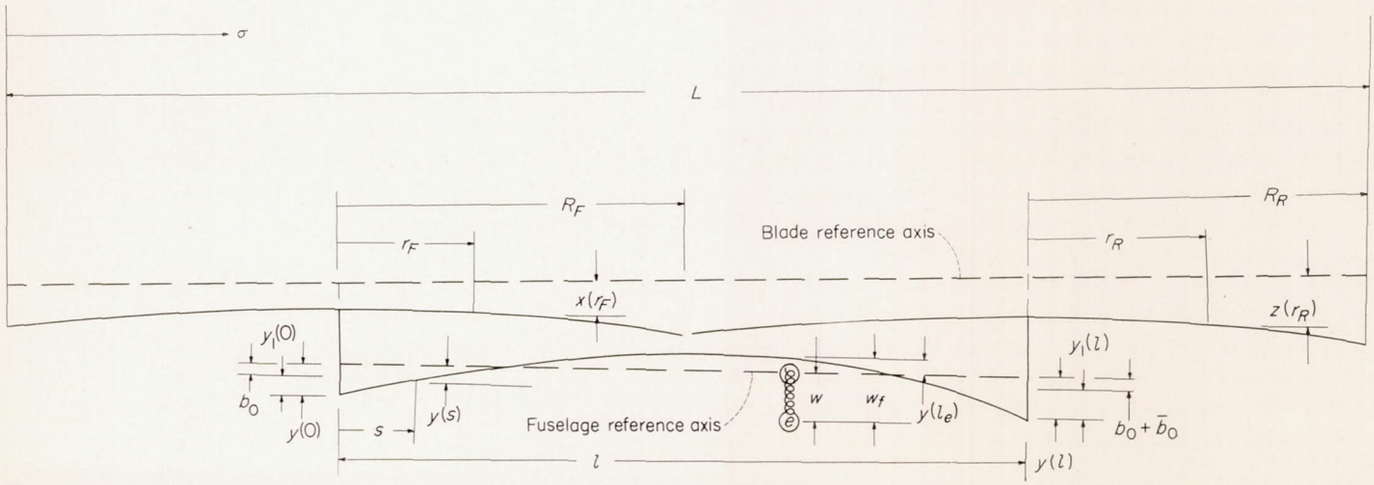

FIGURE II–1.—Coordinates and displacements.

ANALYSIS

EQUATIONS FOR FREE VIBRATIONS

General considerations.—The analysis presented in this portion of the report deals with the determination of the undamped, natural coupled frequencies of the vertical vibrations of a tandem helicopter. The following degrees of freedom are considered: vertical translation, longitudinal pitching, and structural bending of the fuselage; vertical translation, flapping, and flapwise bending of the rotor blades on the front and rear rotors; and vertical translation of the engine. This analysis does not treat fuselage side bending and torsion; however, an analysis of the structure for side bending and torsion can be made in a manner parallel to the present analysis. Although the analysis is given in terms of a tandem helicopter configuration, other configurations may be treated in an analogous manner.

The method follows the Lagrange energy-equation approach wherein the derivation of the equations of motion consists of writing the kinetic and potential energies of the structure in terms of the displacements w, x, y, and z. (See fig. II–1.) These displacements are in terms of generalized coordinates and chosen uncoupled modes of the structural components (fuselage, rotor blades, and engine). The energy equations are substituted in Lagrange's dynamical equations for free vibrations to obtain the equations of motion which yield the coupled frequencies and mode shapes.

Energy equations.—The kinetic energy T and the potential energy V are, respectively,

$$T=\frac{1}{2}\int_0^l m_f\left(\frac{dy}{dt}\right)^2 ds+\frac{1}{2}M_e\left(\frac{dw}{dt}\right)^2+\frac{p}{2}\int_0^{R_F} m_F\left(\frac{dx}{dt}\right)^2 dr_F+\frac{q}{2}\int_0^{R_R} m_R\left(\frac{dz}{dt}\right)^2 dr_R \quad (1)$$

and

$$V=\frac{1}{2}\int_0^l (EI)_f\left(\frac{d^2y}{ds^2}\right)^2 ds+\frac{1}{2}K_e\,[w-y(l_e)]^2+\frac{p}{2}\int_0^{R_F}(EI)_F\left(\frac{d^2x}{dr_F{}^2}\right)^2 dr_F+\frac{q}{2}\int_0^{R_R}(EI)_R\left(\frac{d^2z}{dr_R{}^2}\right)^2 dr_R+\frac{p}{2}\int_0^{R_F} T_F\left(\frac{dx}{dr_F}\right)^2 dr_F+\frac{q}{2}\int_0^{R_R} T_R\left(\frac{dz}{dr_R}\right)^2 dr_R \quad (2)$$

Special attention is called to the fact that the energies of the front rotor with p-blades may be different from those of the rear rotor with q-blades. For this reason, in the derivation of the energies, the deflections of the front and rear rotor blades are denoted independently by x and z, respectively. It is assumed in the present analysis that all the blades on a given rotor behave in a similar manner; however, equations (1) and (2) are readily extended to treat each blade as an independent degree of freedom.

Choice of modes.—The next step toward obtaining the differential equations of motion is to express the deflections w, x, y, and z in terms of chosen mode shapes. The choice of the translation mode, the pitching mode, and one bending mode for the fuselage; the flapping mode and one flapwise bending mode for the blades on each rotor; and one translation mode for the engine leads to the following equations for the deflections:

For engine translation:

$$w=b_0+\bar{b}_0\frac{l_e}{l}+b_1y_1(l_e)+w_f \quad (3)$$

For front-rotor-blade translation, flapping, and bending:

$$x=b_0+b_1y_1(0)+a_0\frac{r_F}{R_F}+a_1x_1 \quad (4)$$

For fuselage translation, pitching, and bending:

$$y=b_0+\bar{b}_0\frac{s}{l}+b_1y_1 \quad (5)$$

For rear-rotor-blade translation, flapping, and bending:

$$z=b_0+\bar{b}_0+b_1y_1(l)+c_0\frac{r_R}{R_R}+c_1z_1 \quad (6)$$

where the coefficients a_0, a_1, b_0, $\bar{b}_0$, b_1, c_0, c_1, and w_f are unknown functions of time, and x_1, y_1, and z_1 are the chosen spatial functions or mode shapes. If higher modes are desired, it is only necessary to add appropriate terms to equations (3) to (6).

Substitution of equations (3) to (6) into equations (1) and (2) leads to the following equations for the kinetic and potential energies, respectively:

$$T=\frac{1}{2}\int_0^l m_f\left(\dot{b}_0+\dot{\bar{b}}_0\frac{s}{l}+\dot{b}_1y_1\right)^2 ds+\frac{1}{2}M_e\left[\dot{b}_0+\dot{\bar{b}}_0\frac{l_e}{l}+\dot{b}_1y_1(l_e)+\dot{w}_f\right]^2+\frac{p}{2}\int_0^{R_F} m_F\left[\dot{b}_0+\dot{b}_1y_1(0)+\dot{a}_0\frac{r_F}{R_F}+\dot{a}_1x_1\right]^2 dr_F+\frac{q}{2}\int_0^{R_R} m_R\left[\dot{b}_0+\dot{\bar{b}}_0+\dot{b}_1y_1(l)+\dot{c}_0\frac{r_R}{R_R}+\dot{c}_1z_1\right]^2 dr_R \quad (7)$$

and

$$V=\frac{1}{2}\int_0^l (EI)_f(b_1y_1'')^2 ds+\frac{1}{2}K_e(w_f)^2+\frac{p}{2}\int_0^{R_F}(EI)_F(a_1x_1'')^2 dr_F+\frac{q}{2}\int_0^{R_R}(EI)_R(c_1z_1'')^2 dr_R+\frac{p}{2}\int_0^{R_F} T_F\left(\frac{a_0}{R_F}+a_1x_1'\right)^2 dr_F+\frac{q}{2}\int_0^{R_R} T_R\left(\frac{c_0}{R_R}+c_1z_1'\right)^2 dr_R \quad (8)$$

where the dots denote derivatives with respect to time and the primes denote derivatives with respect to space or length.

After the energies have been calculated, the next step is to apply Lagrange's equation for free vibration to obtain the differential equations of motion; that is,

$$\left.\begin{aligned}\frac{d}{dt}\left(\frac{\partial T}{\partial\dot{a}_0}\right)-\frac{\partial T}{\partial a_0}+\frac{\partial V}{\partial a_0}=0\\ \frac{d}{dt}\left(\frac{\partial T}{\partial\dot{a}_1}\right)-\frac{\partial T}{\partial a_1}+\frac{\partial V}{\partial a_1}=0\\ \cdot\quad\cdot\quad\cdot\quad\cdot\quad\cdot\end{aligned}\right\} \quad (9)$$

In the application of Lagrange's equation (eqs. (9)), great simplification is obtained if the chosen modes are the natural modes of the uncoupled components; the rest of this report is based on this choice. Equations (7) and (8) are then substituted into equations (9) to obtain the differential equations for free vibration. The characteristic equations for free vibrations are found by considering harmonic motion, that is,

$$\left.\begin{aligned} a_0 &= \tilde{a}_0 \sin \omega t \\ a_1 &= \tilde{a}_1 \sin \omega t \\ &\cdots\cdots \end{aligned}\right\} \tag{10}$$

where the amplitudes of a_0, a_1, . . . are denoted by $\tilde{a}_0$, $\tilde{a}_1$, ... The result of substituting equations (7) and (8) into equations (9) and making use of equations (10) leads to the characteristic equations which are given in matrix form as follows:

$$\begin{bmatrix}
M_f+M_e+pM_F+qM_R & M_e\frac{l_e}{l}+qM_2+M_f\frac{l_{cg}}{l} & A_0 & B_0 & M_e y_1(l_e)+pM_F y_1(0)+qM_R y_1(l) & A_1 & B_1 & M_e \\
M_e\frac{l_e}{l}+qM_R+M_f\frac{l_{cg}}{l} & M_f\left(\frac{k}{l}\right)^2+M_e\left(\frac{l_e}{l}\right)^2+qM_R & 0 & B_0 & M_e\frac{l_e}{l}y_1(l_e)+qM_R y_1(l) & 0 & B_1 & M_e\frac{l_e}{l} \\
A_0 & 0 & C_0\left[1-\left(\frac{\Omega}{\omega}\right)^2\right] & 0 & y_1(0)A_0 & 0 & 0 & 0 \\
B_0 & B_0 & 0 & D_0\left[1-\left(\frac{\Omega}{\omega}\right)^2\right] & y_1(l)B_0 & 0 & 0 & 0 \\
pM_F y_1(0)+qM_R y_1(l)+M_e y_1(l_e) & M_e\frac{l_e}{l}y_1(l_e)+qM_R y_1(l) & y_1(0)A_0 & y_1(l)B_0 & \left[1-\left(\frac{\omega_{f,1}}{\omega}\right)^2\right]M_{f,1}+M_e y_1^2(l_e)+pM_F y_1^2(0)+qM_R y_1^2(l) & y_1(0)A_1 & y_1(l)B_1 & M_e y_1(l_e) \\
A_1 & 0 & 0 & 0 & y_1(0)A_1 & C_1\left[1-\left(\frac{\omega_{F,1}}{\omega}\right)^2-K_{F,1}\left(\frac{\Omega}{\omega}\right)^2\right] & 0 & 0 \\
B_1 & B_1 & 0 & 0 & y_1(l)B_1 & 0 & D_1\left[1-\left(\frac{\omega_{R,1}}{\omega}\right)^2-K_{R,1}\left(\frac{\Omega}{\omega}\right)^2\right] & 0 \\
M_e & M_e\frac{l_e}{l} & 0 & 0 & M_e y_1(l_e) & 0 & 0 & M_e\left[1-\left(\frac{\omega_e}{\omega}\right)^2\right]
\end{bmatrix}
\begin{Bmatrix} \tilde{b}_0 \\ \tilde{\tilde{b}}_0 \\ \tilde{a}_0 \\ \tilde{c}_0 \\ \tilde{b}_1 \\ \tilde{a}_1 \\ \tilde{c}_1 \\ \tilde{w}_f \end{Bmatrix} = 0 \tag{11}$$

where

$$A_0=\frac{p}{R_F}\int_0^{R_F} m_F r_F\,dr_F \qquad B_0=\frac{q}{R_R}\int_0^{R_R} m_R r_R\,dr_R$$

$$A_1=p\int_0^{R_F} m_F x_1\,dr_F \qquad B_1=q\int_0^{R_R} m_R z_1\,dr_R$$

$$C_0=\frac{p}{R_F{}^2}\int_0^{R_F} m_F r_F{}^2\,dr_F \qquad D_0=\frac{q}{R_R{}^2}\int_0^{R_R} m_R r_R{}^2\,dr_R$$

$$C_1=p\int_0^{R_F} m_F x_1{}^2\,dr_F \qquad D_1=q\int_0^{R_R} m_R z_1{}^2\,dr_R$$

$$K_{F,1}=\frac{p}{C_1}\int_0^{R_F} \overline{T}_F(x_1')^2\,dr_F \qquad K_{R,1}=\frac{q}{D_1}\int_0^{R_R} \overline{T}_R(z_1')^2\,dr_R$$

$$M_{f,1}=\int_0^{l} m_f y_1{}^2\,ds \qquad \omega_e{}^2=\frac{K_e}{M_e}$$

In the abbreviated notation used in the appendix, equation (11) can be written as

$$[H]\{\eta\}=0 \tag{11a}$$

COUPLED FREQUENCIES AND MODE SHAPES

The values of ω, the natural frequencies of the coupled modes of the helicopter, are determined by setting the determinant of equation (11) equal to zero. The coupled mode shapes are determined by substitution of the modal coefficients $\tilde{b}_0$, $\tilde{\tilde{b}}_0$, and so forth, obtained from equation (11), into equations (3) to (6).

Inspection of equation (11) reveals that, although there are eight degrees of freedom, the frequency term ω appears in only six of the diagonal terms when $\Omega\neq 0$ and in only four of the diagonal terms when $\Omega=0$. Thus, the amount of work involved in the solution of the determinant can be reduced by changing the order of the matrix from eight to six when $\Omega\neq 0$ and from eight to four when $\Omega=0$. The steps involved in this transformation as well as the final matrices obtained for $\Omega=30$ radians per second and $\Omega=0$ for the basic configuration are given in the appendix. The appendix also contains some pertinent remarks regarding methods for obtaining the modal coefficients.

EQUATIONS FOR RESPONSE OF HELICOPTER TO APPLIED LOADS

Once the natural frequencies and shapes of the coupled modes are obtained, the next objective is to determine the response of the helicopter to applied aerodynamic loads. The calculation of the response necessitates a consideration of the damping of the structure. In the analysis that follows, a method is presented which permits the coupled mode shapes and frequencies determined by the methods presented in previous sections of this report to be utilized, with the inclusion of structural damping, in the determination of the response of the helicopter to arbitrary forces.

If $\phi(\sigma, t)$ be designated as the deflection of the helicopter at station σ at time t (fig. II–1), the differential equation of motion for an element of the helicopter at station σ is

$$(1+ig_h)\frac{\partial^2}{\partial\sigma^2}\left(EI\frac{\partial^2\phi}{\partial\sigma^2}\right)+m\ddot{\phi}=F(\sigma,t) \tag{12}$$

where F is the applied force, g_h is the conventional structural damping coefficient, and simple harmonic motion is implied. If it is assumed that the total deflection can be expressed as a superposition of the natural coupled modes of the structure, then

$$\phi(\sigma,t)=\sum_{r=1}^{r=n}\alpha_r(t)\phi_r(\sigma) \tag{13}$$

where $\phi_r(\sigma)$ is the rth-coupled-mode shape and $\alpha_r(t)$ is the time-dependent coefficient of the rth mode. Substitution of equation (13) into equation (12) yields

$$(1+ig_h)\alpha_1(t)\frac{\partial^2}{\partial\sigma^2}\left(EI\frac{\partial^2\phi_1}{\partial\sigma^2}\right)+(1+ig_h)\alpha_2(t)\frac{\partial^2}{\partial\sigma^2}\left(EI\frac{\partial^2\phi_2}{\partial\sigma^2}\right)+$$
$$\ldots+(1+ig_h)\alpha_n(t)\frac{\partial^2}{\partial\sigma^2}\left(EI\frac{\partial^2\phi_n}{\partial\sigma^2}\right)=-\ddot{\alpha}_1(t)m\phi_1-$$
$$\ddot{\alpha}_2(t)m\phi_2-\ldots-\ddot{\alpha}_n(t)m\phi_n+F(\sigma,t) \tag{14}$$

Since the natural modes of vibration are defined by

$$\frac{\partial^2}{\partial\sigma^2}\left(EI\frac{\partial^2\phi_r}{\partial\sigma^2}\right)=\omega_r{}^2m\phi_r \tag{15}$$

equation (14) can be written as

$$(1+ig_h)\alpha_1(t)\omega_1{}^2m\phi_1+(1+ig_h)\alpha_2(t)\omega_2{}^2m\phi_2+\ldots+$$
$$(1+ig_h)\alpha_n(t)\omega_n{}^2m\phi_n=-\ddot{\alpha}_1(t)m\phi_1-\ddot{\alpha}_2(t)m\phi_2-\ldots-$$
$$\ddot{\alpha}_n(t)m\phi_n+F(\sigma,t) \tag{16}$$

Upon multiplication of equation (16) by ϕ_r, integrating over the length, and observing the conditions of orthogonality for natural modes, namely,

$$\left.\begin{aligned}\int_0^L m\phi_r\phi_s d\sigma=0 \qquad (r\neq s)\\ \int_0^L m\phi_r\phi_s d\sigma=M_r \qquad (r=s)\end{aligned}\right\} \tag{17}$$

equation (16) becomes

$$(1+ig_h)\alpha_r\omega_r{}^2M_r=-\ddot{\alpha}_rM_r+\int_0^L F(\sigma,t)\phi_r d\sigma \tag{18}$$

In general, F will be a distributed force and, if necessary, the integral term of equation (18) can be evaluated. For purposes of illustration, however, it is assumed that F is a concentrated force and the rest of the analysis is based on that assumption. The integral term of equation (18) is

$$\int_0^L F(\sigma,t)\phi_r d\sigma=F\phi_r(\sigma_A) \tag{19}$$

where F is the force applied and $\phi_r(\sigma_A)$ is the deflection of the rth mode at the point of application of the force. Therefore,

$$(1+ig_h)\alpha_r\omega_r{}^2M_r+\ddot{\alpha}_rM_r=F\phi_r(\sigma_A) \tag{20}$$

If α_r and F are expressed as the real parts of $\alpha_{r,0}e^{i\omega t}$ and $F_0e^{i\omega t}$, respectively, then

$$(1+ig_h)\alpha_{r,0}\omega_r{}^2M_r-\omega^2\alpha_{r,0}M_r=F_0\phi_r(\sigma_A) \tag{21}$$

The amplitude of α_r is

$$\alpha_{r,0}=\frac{\frac{F_0\phi_r(\sigma_A)}{\omega_r{}^2M_r}}{\left[1-\left(\frac{\omega}{\omega_r}\right)^2\right]+ig_h} \tag{22}$$

and, by definition, the coefficient of the motion in the rth mode is given by the real part of the following expression:

$$\alpha_r=\frac{\frac{F_0\phi_r(\sigma_A)}{\omega_r{}^2M_r}}{\left[1-\left(\frac{\omega}{\omega_r}\right)^2\right]+ig_h}e^{i\omega t}=(P_r-iQ_r)e^{i\omega t} \tag{23}$$

where

$$\left.\begin{aligned}P_r&=\frac{\frac{F_0\phi_r(\sigma_A)}{\omega_r{}^2M_r}}{\left[1-\left(\frac{\omega}{\omega_r}\right)^2\right]^2+g_h{}^2}\left[1-\left(\frac{\omega}{\omega_r}\right)^2\right]\\ Q_r&=\frac{\frac{F_0\phi_r(\sigma_A)}{\omega_r{}^2M_r}}{\left[1-\left(\frac{\omega}{\omega_r}\right)^2\right]^2+g_h{}^2}g_h\end{aligned}\right\} \tag{24}$$

Substitution of equation (23) into equation (13) yields the total response ϕ

$$\phi(\sigma,t)=\left[\sum_{r=1}^{r=n}(P_r-iQ_r)\phi_r\right]e^{i\omega t} \tag{25}$$

the amplitude of which is

$$|\phi|=\sqrt{\left(\sum_{r=1}^{r=n}P_r\phi_r\right)^2+\left(\sum_{r=1}^{r=n}Q_r\phi_r\right)^2}=\sqrt{X^2+Y^2} \tag{26}$$

Then $|\phi|$ is the amplitude of vibration at any station σ in response to a harmonic force, applied at $\sigma=\sigma_A$, which has an amplitude F_0 and a frequency ω. It should be noted in the application of equation (26) that $\phi_1, \phi_2, \ldots \phi_n$ are the values of the coupled modes at station σ.

In the event that it is desired that the response at any station be calculated for loads applied at several different stations, then some reduction of the work required may be obtained by suitably modifying the coefficients P_r and Q_r. Assume, for example, that $(P_r)_{\mathrm{I}}$ and $(Q_r)_{\mathrm{I}}$ are the in-phase and out-of-phase components of the response in the rth mode to an oscillating load applied at the front hub and designated by subscript I. From equation (26), the response in the rth mode at the same station to a load of the same magnitude applied in the same direction at the rear hub, and designated by subscript II, is given by the components:

$$\left.\begin{aligned}(P_r)_{\mathrm{II}}&=(P_r)_{\mathrm{I}}\phi_r(\sigma_A)_{\mathrm{II}}/\phi_r(\sigma_A)_{\mathrm{I}}\\ (Q_r)_{\mathrm{II}}&=(Q_r)_{\mathrm{I}}\phi_r(\sigma_A)_{\mathrm{II}}/\phi_r(\sigma_A)_{\mathrm{I}}\end{aligned}\right\} \tag{27}$$

The in-phase and out-of-phase components of the response due to all the modes is then given by

$$\left.\begin{aligned}X_{\mathrm{II}}&=\sum_{r=1}^{r=n}(P_r)_{\mathrm{II}}\phi_r\\ Y_{\mathrm{II}}&=\sum_{r=1}^{r=n}(Q_r)_{\mathrm{II}}\phi_r\end{aligned}\right\} \tag{28}$$

The response due to any combination of forces applied at either or both hubs in the same or opposite directions is then obtained by adding X_{I}, X_{II}, Y_{I}, and Y_{II} in the proper sense and proportions.

DISCUSSION OF RESULTS

CALCULATION OF COUPLED FREQUENCIES AND MODE SHAPES

Scope of the calculations.—The analysis derived in this report was used to calculate the natural coupled frequencies of a tandem helicopter having the structural parameters given in table II–1. The resulting modal coefficients are given in table II–2 and the natural frequencies and mode shapes are given in figures II–2 and II–3. Some additional calculations were made to evaluate the effects of the natural frequency of the uncoupled fuselage system and the Southwell coefficient of the blades on the natural frequencies of the coupled system. These results are shown in figures II–4 and II–5. Calculations were also made for a three-degree-of-freedom system (bending of the fuselage and bending of the blades on the front and rear rotors) and the resulting frequencies are compared with appropriate frequencies for the eight-degree-of-freedom system in figure II–6 to obtain some idea of the relative contributions of the various degrees of freedom to the overall problem.

TABLE II–1.—PARAMETERS USED IN CALCULATIONS

(a) Blade parameters (blades on front and rear rotor assumed to be identical)

[$\omega_{F,1}=\omega_{R,1}=25.3$ radians/sec; $K_{F,1}=K_{R,1}=6.2$; $R_F=R_R=210$ in.; $p=q=3$; $M_F=M_R=0.194$ lb-sec^2/in.]

Station	Radial location, r_F or r_R, in.	Mass distribution, m_F or m_R, lb-sec^2/in.^{2}	First-bending mode shape, x_1 or z_1 (nondimensionalized)
1	10.5	3.03×10^{-3}	−0.09
2	31.5	1.52	−.27
3	52.5	.67	−.42
4	73.5	.59	−.50
5	94.5	.59	−.53
6	115.5	.53	−.50
7	136.5	.45	−.34
8	157.5	.40	−.07
9	178.5	.50	.28
10	199.5	.59	.75

(b) Fuselage and engine parameters

[$\omega_{f,1}=89.2$ radians/sec; $\omega_e=130$ radians/sec; $M_e=2.861$ lb-sec^2/in.; $l_e/l=0.735$]

Station	Fuselage location, s/l	Length of fuselage element, Δs, in.	Mass of fuselage element, $m_f\Delta s$, lb-sec^2/in.	First-bending mode shape, y_1 (nondimensionalized)
1	0	32.44	1.28	0.76
2	.123	32.44	1.98	.36
3	.250	32.44	.42	.03
4	.375	32.44	.86	−.21
5	.500	32.44	2.12	−.36
6	.625	24.46	.80	−.38
7	.735	40.42	.23	−.27
8	.875	32.44	.81	.26
9	1.000	32.44	1.58	1.00

TABLE II–2.—MODAL COEFFICIENTS

	Modal coefficients for natural frequencies—					
	ω_1	ω_2	ω_3	ω_4	ω_5	ω_6
			$\Omega=0$			
$\tilde{b}_0$	----------	----------	−2.362	86.36	−0.02010	0.02635
$\tilde{\tilde{b}}_0$	----------	----------	−0.6313	−157.3	0.1598	−1.736
$\tilde{a}_0$	----------	----------	2.652	−144.2	−1.224	−1.301
$\tilde{c}_0$	----------	----------	3.299	115.7	−1.886	1.174
$\tilde{b}_1$	----------	----------	1	1	1	1
$\tilde{a}_1$	----------	----------	−182.1	2,802	1.043	1.032
$\tilde{c}_1$	----------	----------	−226.5	−2,250	1.607	−0.9300
$\tilde{w}_f$	----------	----------	−0.1233	−1.212	−0.1182	4.266
			$\Omega=20$ radians/sec			
$\tilde{b}_0$	−3.925	123.1	−0.2716	32.21	−0.01219	0.03148
$\tilde{\tilde{b}}_0$	−0.9383	−225.3	−0.04228	−56.51	0.1701	−1.748
$\tilde{a}_0$	153.4	−2,183	−0.9310	−62.22	−1.310	−1.330
$\tilde{c}_0$	187.5	1,782	−1.308	43.95	−2.028	1.204
$\tilde{b}_1$	1	1	1	1	1	1
$\tilde{a}_1$	0.6192	−26.11	−21.40	1,060	1.684	1.148
$\tilde{c}_1$	0.7558	21.31	−30.06	43.95	2.608	−1.040
$\tilde{w}_f$	−0.1227	−1.146	−0.1252	−2.282	−0.1171	4.273
			$\Omega=30$ radians/sec			
$\tilde{b}_0$	−1.552	62.72	−0.07493	35.59	0.009242	0.04096
$\tilde{\tilde{b}}_0$	−0.4512	−113.6	0.09865	−60.30	0.2010	−1.775
$\tilde{a}_0$	61.00	−1,123	−1.369	−69.86	−1.425	−1.366
$\tilde{c}_0$	77.30	881.8	−2.045	45.57	−2.242	1.266
$\tilde{b}_1$	1	1	1	1	1	1
$\tilde{a}_1$	0.1760	−15.41	−4.654	1,188	3.734	1.389
$\tilde{c}_1$	0.2225	12.11	−6.968	−776.4	5.883	−1.274
$\tilde{w}_f$	−0.1239	−1.312	−0.1223	−5.586	−0.1128	4.293

Frequencies and mode shapes for the basic configuration.—The basic configuration is designated by the parameters given in table II–1 which correspond closely to those of an existing tandem helicopter. The natural frequencies and mode shapes of the coupled system were calculated for this configuration for three rotor speeds: namely, 0, 20, and 30 radians per second. The natural frequencies are plotted in figure II–2 as a function of rotor speed, and the modal coefficients are tabulated in table II–2 for each of the six natural frequencies and for each of the three rotor speeds. A rotor speed of 30 radians per second corresponds very closely to the normal operating rotor speed for the chosen helicopter. The modal coefficients presented in table II–2 for this speed were used in equations (3) to (6) to obtain the mode shapes which are presented in figure II–3 and which are also sketched in figures II–2, II–4, and II–5 to identify the modes of vibration that correspond to the different natural frequencies of the coupled system.

The effect of coupling of the various degrees of freedom on the natural frequencies is indicated in figure II–2 by a comparison of the coupled frequencies (shown by solid lines) with the uncoupled frequencies (shown by short-dashed lines). The curve for uncoupled blade first bending represents the blades of both the front and rear rotors. There are also short-dashed curves for uncoupled blade flapping; however, these curves cannot be seen inasmuch as they are coincident with the frequency curve for the lower coupled mode. The frequencies of the 2- and 3-per-revolution harmonic component of the aerodynamic loading (designated 2–P and 3–P herein and indicated by the long-dashed lines in fig. II–2) are also presented to permit comparison

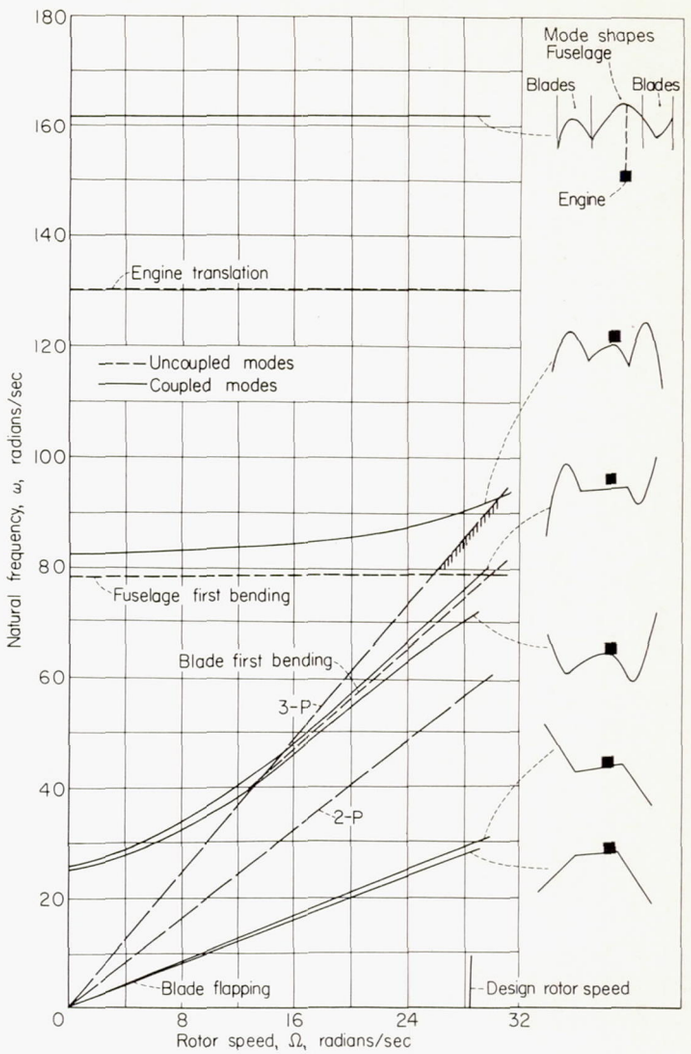

FIGURE II–2.—Variation of natural frequencies with rotor speed.

with the natural frequencies. With the exception of the engine translational frequency and the fuselage first-bending frequency, the differences between the coupled and uncoupled frequencies are negligible at low rotor speeds. As the rotor speed is increased, the uncoupled frequencies of the fuselage mode and the blade bending modes approach each other, and, as expected, the effects of coupling become pronounced.

The helicopter used as an example for these calculations has three blades on each rotor, and, therefore, the 3–P components of the aerodynamic loading on the rotor blades are additive at the respective hubs. Thus, the region of primary importance on the frequency diagram of figure II–2 is the region at or near the crosshatched marks on the 3–P line which brackets the normal variation of the design rotor speed.

Inasmuch as the two rotors rotate in opposite directions with a phase difference of blade position on the two rotors of approximately 60°, blades from both rotors are advancing into the wind simultaneously three times per revolution of each rotor. This condition suggests that the resultant 3–P periodic forces at the two hubs are in phase and would be particularly effective in the excitation of the symmetrical

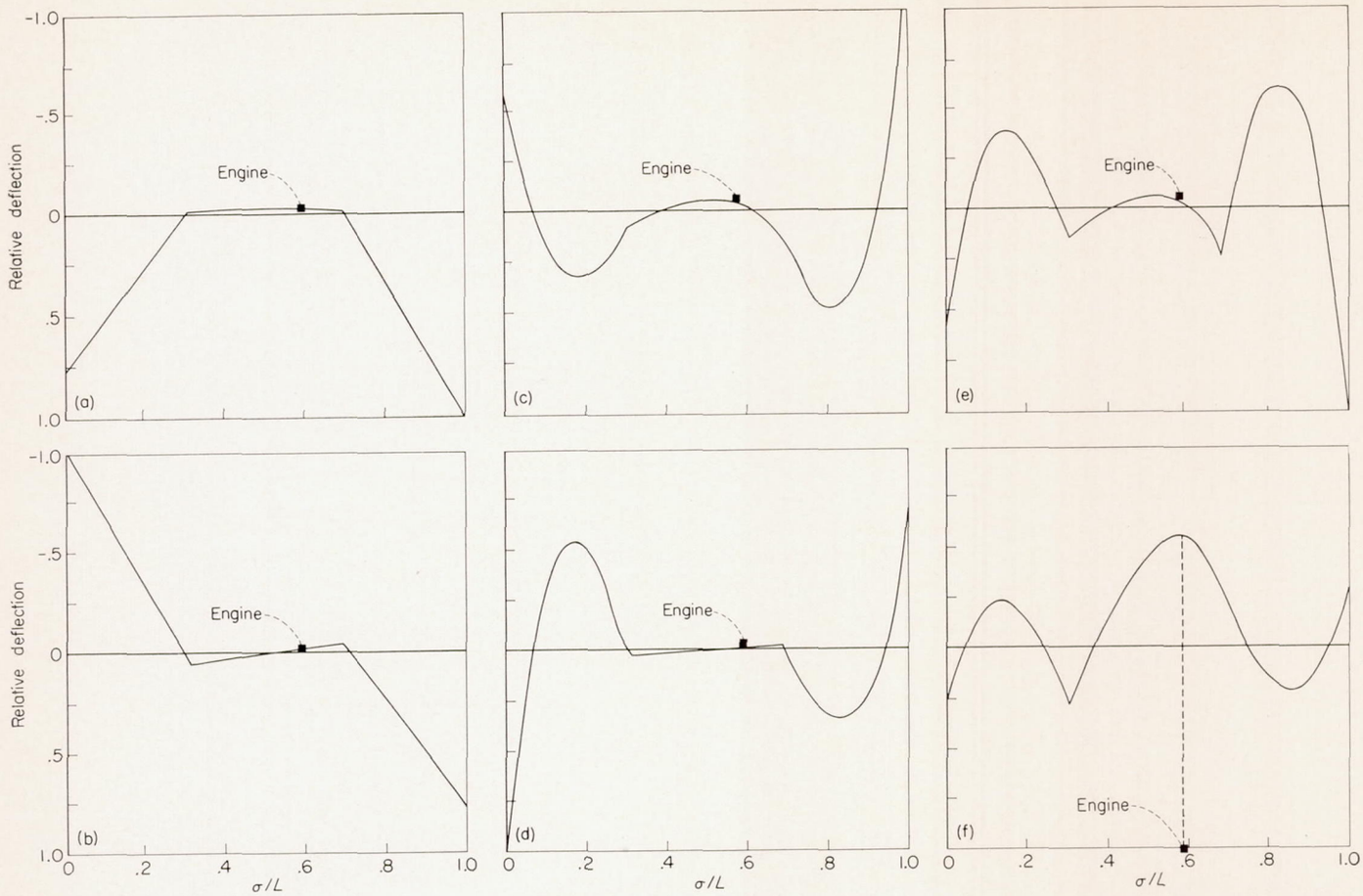

(a) First-coupled-mode shape.
(b) Second-coupled-mode shape.
(c) Third-coupled-mode shape.
(d) Fourth-coupled-mode shape.
(e) Fifth-coupled-mode shape.
(f) Sixth-coupled-mode shape.

FIGURE II–3.—Mode shapes of coupled rotor-fuselage system.

modes of the helicopter which have natural frequencies in the general region of 85 radians per second. Figure II–2 shows that there are three coupled modes of the helicopter which have natural frequencies reasonably close to the 3–P frequency, two of which are symmetrical and the other antisymmetrical. In view of the preceding discussion, the data of figure II–2 indicate that at the higher rotor speed (30 radians per second) the response of this helicopter in the third symmetrical mode to the 3–P oscillating excitation forces would be increased substantially by resonance amplification. Furthermore, if there is a component of the 3–P aerodynamic loading at the two rotor hubs which is out of phase, it appears likely that the structural response in the second antisymmetrical mode would also be increased by resonance amplification.

The mode shapes presented in figure II–3 show that the mode shapes alternate between symmetrical and antisymmetrical configurations. The relative motion of the engine with respect to the fuselage is shown to be negligible for the lower frequency modes but becomes relatively large at the highest frequency mode (sixth-coupled-mode shape).

EFFECT OF VARIATIONS IN UNCOUPLED COMPONENTS

Effect of natural uncoupled frequency of the fuselage.—The analysis presented in this report permits the inclusion of the natural uncoupled frequency of the fuselage as one of the parameters. This frequency can be calculated by analytical methods such as those of references 1 and 2; however, this requires an accurate knowledge of the mass and stiffness distribution of the fuselage which may be difficult to obtain. The accuracy to which this frequency can be obtained experimentally for a given helicopter depends upon such considerations as the manner of support and the type of shaker installation. Since this frequency is one of the primary parameters, it is of interest to determine to what extent the natural frequencies of the coupled modes are changed by variations of the uncoupled frequency of the fuselage. Conversely, if the natural frequencies of the coupled system for a known design value of the natural uncoupled frequency of the fuselage are of such a magnitude as to lead to resonance amplification of the structural response, it is desirable to evaluate the extent to which the coupled frequencies can be changed by varying the uncoupled frequency of the fuselage.

An indication of the change in the natural frequencies of the coupled modes due to changes in the uncoupled frequency of the fuselage is shown by the curves of figure II–4. The calculations show that the frequencies of the second and third symmetrical modes are changed appreciably whereas the frequencies of the antisymmetrical modes are not affected. Since the amount of fuselage bending in the antisymmetrical modes is negligible in comparison with the amount of fuselage bending in the symmetrical modes, the

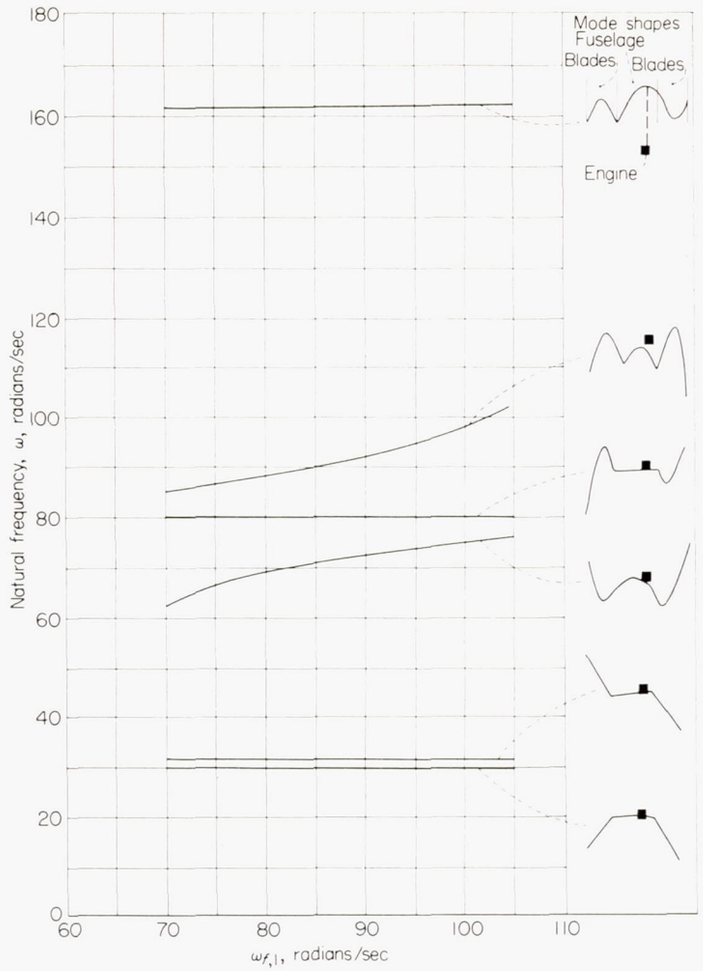

FIGURE II–4.—Effect of natural uncoupled frequency of fuselage on natural frequencies of coupled system. $\Omega=30$ radians per second.

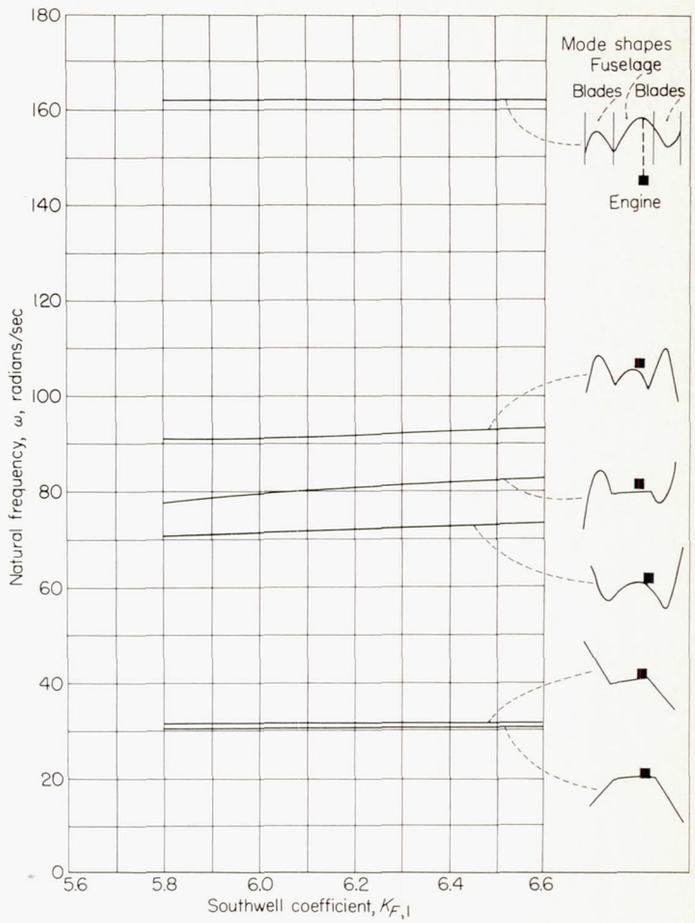

FIGURE II–5.—Effect of Southwell coefficient for blade first elastic flapwise bending on natural frequencies of coupled system. $\Omega=30$ radians per second.

results shown in figure II–4 are in agreement with expectations.

Effect of Southwell coefficient for the blade first elastic flapwise bending mode.—The value of the Southwell coefficient chosen for the blade first elastic flapwise bending mode has a direct effect on the uncoupled frequency of the rotating blade. An indication of the effect of this parameter on the coupled frequencies is shown in figure II–5. The value of $K_{F,1}$ estimated by means of reference 4 for the blade considered is 6.2 and the range of values chosen for these calculations is believed to be more than adequate to allow for estimation errors. These calculations show that the coupled frequencies of both the symmetrical and antisymmetrical modes which have frequencies approximately equal to the uncoupled blade-bending frequencies are increased slightly as the Southwell coefficient is increased, and that errors in the values of the coupled frequencies due to the estimation of the Southwell coefficient $K_{F,1}$ should not exceed 2 or 3 percent.

COMPARISON OF RESULTS OF THREE-MODE AND EIGHT-MODE ANALYSIS

Figure II–2 shows that the uncoupled modes which are primarily affected by coupling in the frequency region of the 3–P excitation forces are fuselage bending and the bending of the blades on the front and rear rotors. Calculations were made to determine how well the frequencies of the coupled modes could be predicted by using only these three uncoupled modes. The calculation procedure consisted of retaining only the fifth, sixth, and seventh rows and columns of the frequency determinant of equation (11). The results are given in figure II–6 together with the corresponding frequencies obtained from the eight-mode analysis. A comparison of the frequencies for the two cases shows that the frequencies calculated by the three-mode analysis are from 3 to 6 percent lower than those obtained by the eight-mode analysis, and suggests that a three-mode analysis might be useful for obtaining a first approximation of the coupled frequencies in this region for configurations similar to the one treated herein.

CALCULATION OF THE RESPONSE OF THE HELICOPTER TO APPLIED LOADS

The methods developed in the previous sections of this report were applied to calculate the amplitudes of the response of the helicopter at the location of the cockpit for harmonic oscillating forces applied at the front and rear rotor hubs. The amplitudes of vibration were calculated as a function of frequency of the periodic force for one value of damping ($g_h=0.1$) and at a rotor speed of 30 radians per second for the four cases which follow:

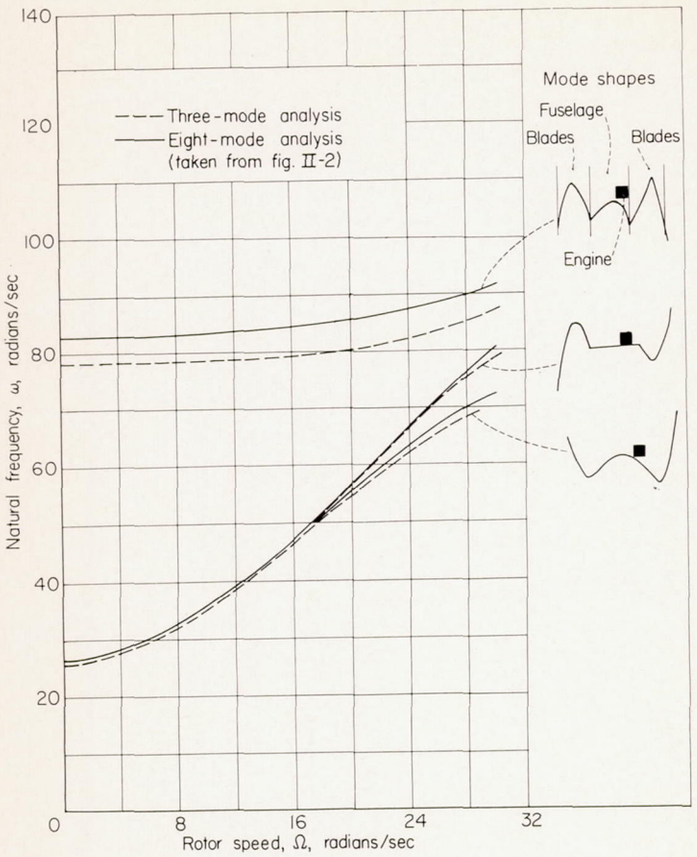

FIGURE II–6.—Comparison of natural frequencies of coupled system from three-mode analysis with corresponding frequencies from eight-mode analysis.

Case I: Oscillating force of unit magnitude applied in a vertical direction at the front rotor hub.

Case II: Oscillating force of unit magnitude applied in a vertical direction at the rear rotor hub.

Case III: Oscillating force of one-half unit magnitude applied in a vertical direction at both the front and rear rotor hubs in the same direction.

Case IV: Oscillating force of one-half unit magnitude applied in a vertical direction at the front and rear rotor hubs in opposite directions (producing a pure pitching moment on the fuselage).

The in-phase and out-of-phase components of the response, or cockpit deflections, are given in figures II–7 and II–8 as a function of frequency for cases I and II, respectively. The natural coupled frequencies are indicated by the vertical dashed lines at the bottom of the figures. The response curves are presented to familiarize the reader with the nature of the components and as an aid in the calculation of the cockpit deflections due to other combinations of loads at the front and rear rotor hubs. The cockpit deflections for cases III and IV as well as for cases I and II were obtained by suitably combining the in-phase and out-of-phase components of figures II–7 and II–8 as outlined in the analysis section.

The amplitude of the cockpit vibrations resulting from the oscillating forces applied to the hub in the four cases previously outlined are given in figures II–9 to II–12, respectively. Before discussing these figures, the reader's attention is again directed to figure II–2 where, at the rotor speed of 30 radians per second for which these response calculations are appropriate, six distinct natural frequencies are indicated within the range from 0 to 180 radians per second. These natural frequencies are indicated by the vertical dashed lines at the bottom of figures II–9 to II–12. For the hypothetical case of zero damping, it is expected then that the response curves similar to those of figures II–9 to II–12 would indicate six peaks of infinite amplitude at frequencies corresponding to the natural frequencies. With the inclusion of a small amount of damping, these peaks become finite and as the damping is progressively increased some of the peaks disappear. The peaks which remain when the forces are applied in a given manner indicate the modes in which the given forces are more effective in doing work.

The curves of figures II–9 to II–12 show the responses obtained for $g_h=0.1$ for the four cases investigated. The manner of application of the load in each case is indicated in the figure by the accompanying sketch of a tandem helicopter. In a few instances where the number of calculated points, indicated by the small circles, are insufficient to define the peaks completely, the peaks are indicated by the long-dashed lines. All the figures indicate peaks at frequencies of approximately 32, 72, and 92 radians per second and show that the coupled modes which contribute most to the responses are the second, third, and fifth coupled modes, respectively, of figure II–3. This effect was also observed during the calculations by inspection of the values of the individual values of P_r and Q_r. (See eq. (24)). The most significant deviation from the general trend of high responses at forcing frequencies near the natural frequencies of the aforementioned coupled modes is found in figure II–12. In this case, the response to forces applied so as to produce a moment on the helicopter is found to diminish considerably at the higher forcing frequencies. This reduction of the response at the higher frequencies appears significant because it indicates that, if the aerodynamic forcing functions which are usually encountered in flight could be forced to occur in an antisymmetric manner, the response at a frequency of 3–P or 90 radians per second would be substantially reduced over that obtained for symmetrically applied loadings as shown by figure II–11.

Perhaps one of the most significant points brought out by these studies is the fact that it is not always possible to obtain the natural frequencies of all the coupled modes of a structure by observing the response of the structure to arbitrary inputs. Conversely, if the applied loads are realistically chosen to be representative of those encountered under normal flight conditions, the peaks of the response curve appear to give fairly good indications of the natural frequencies of the more important coupled modes.

CONSIDERATIONS REGARDING FURTHER REFINEMENT OF THE METHOD

The studies presented in this report—although believed to be useful in the evaluation and reduction of the critical vibrations of tandem helicopters by emphasizing the importance of coupled natural frequencies and mode shapes, providing a method for estimating them, and, in turn, using them to determine the response of the helicopter to applied loads—do not provide a complete answer to the problem.

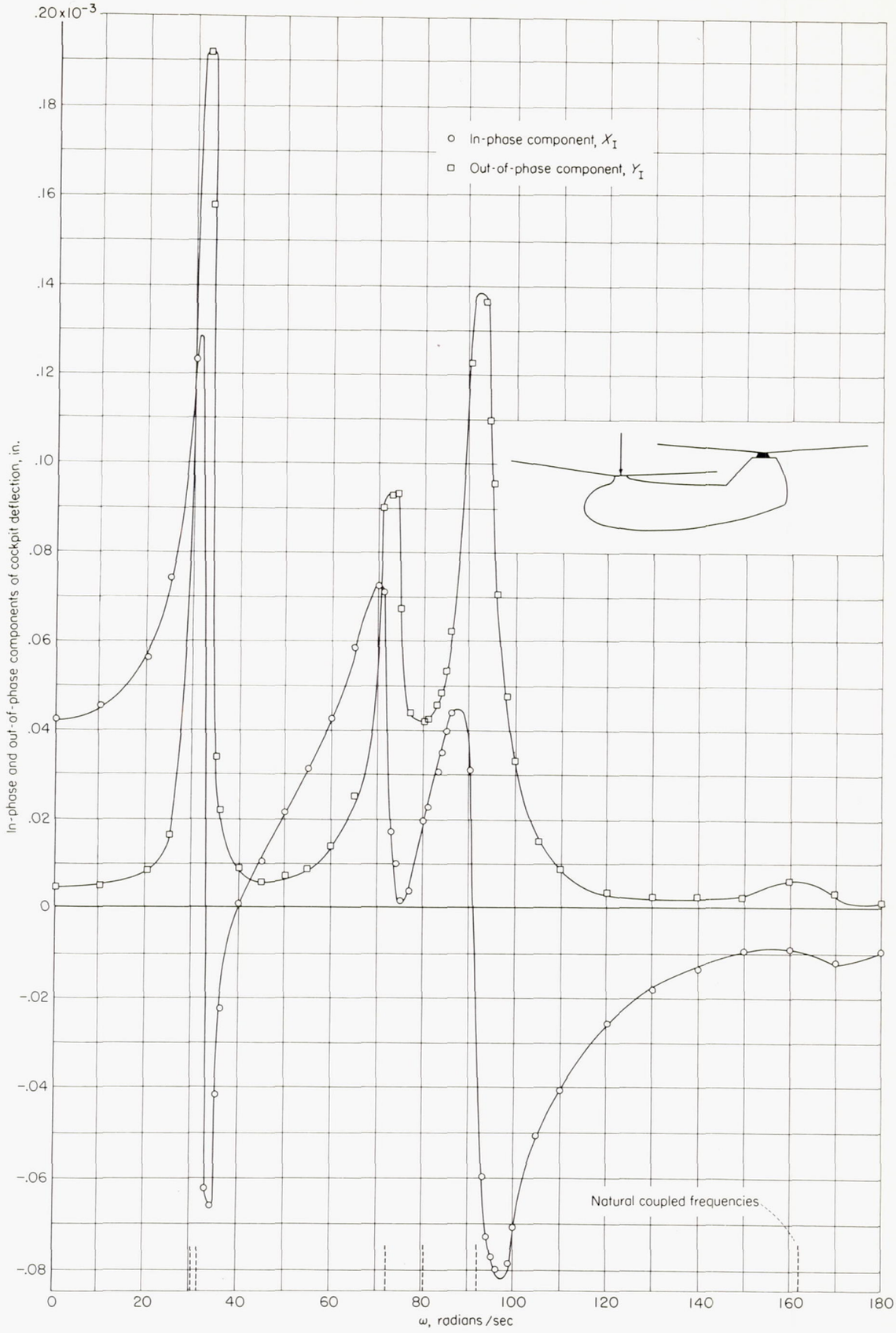

FIGURE II–7.—Effect of forcing frequency on in-phase and out-of-phase components of amplitude of vibration of cockpit. Oscillating force of unit magnitude applied at front rotor hub.

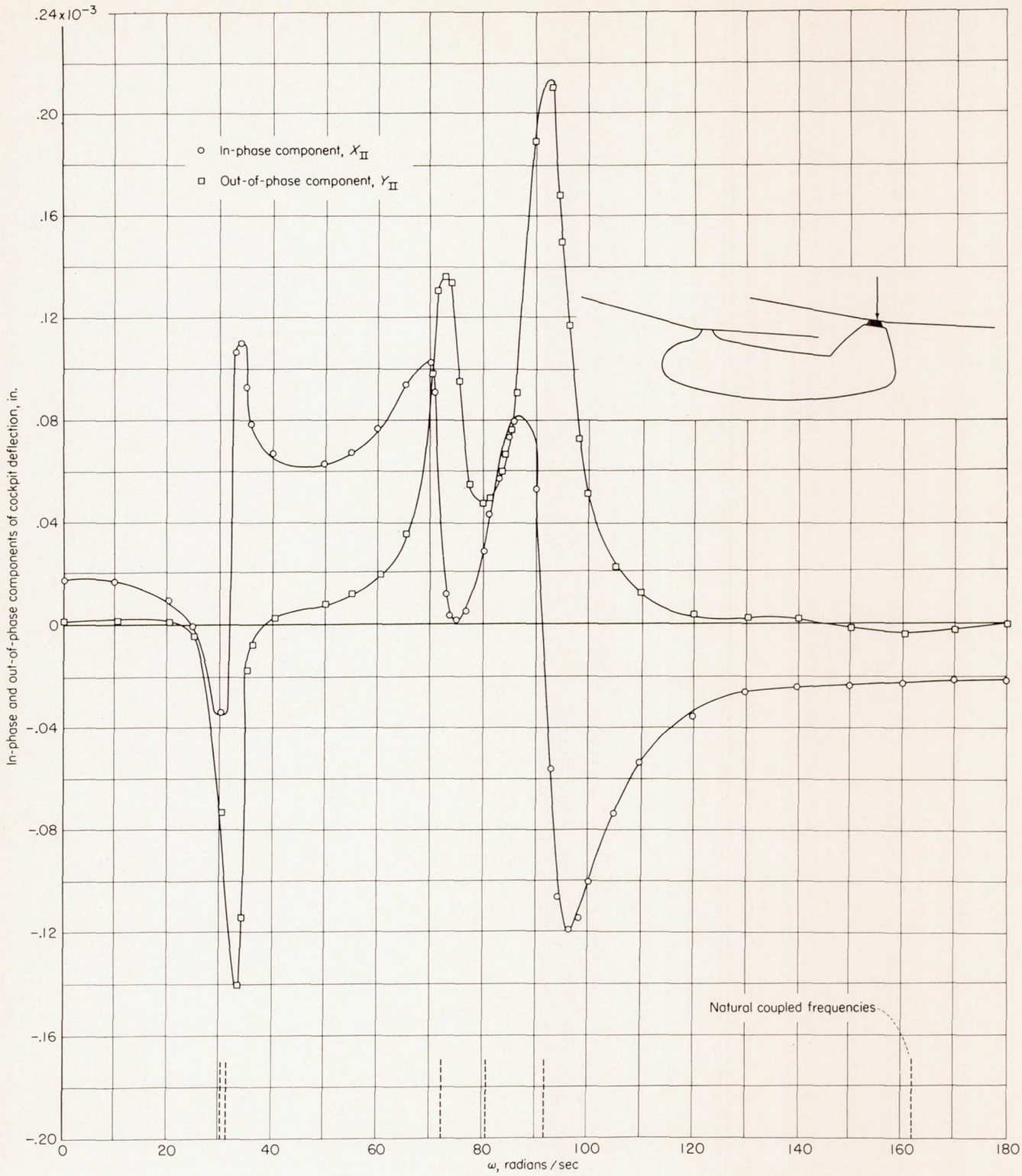

FIGURE II–8.—Effect of forcing frequency on in-phase and out-of-phase components of amplitude of vibration of cockpit. Oscillating force of unit magnitude applied at rear rotor hub.

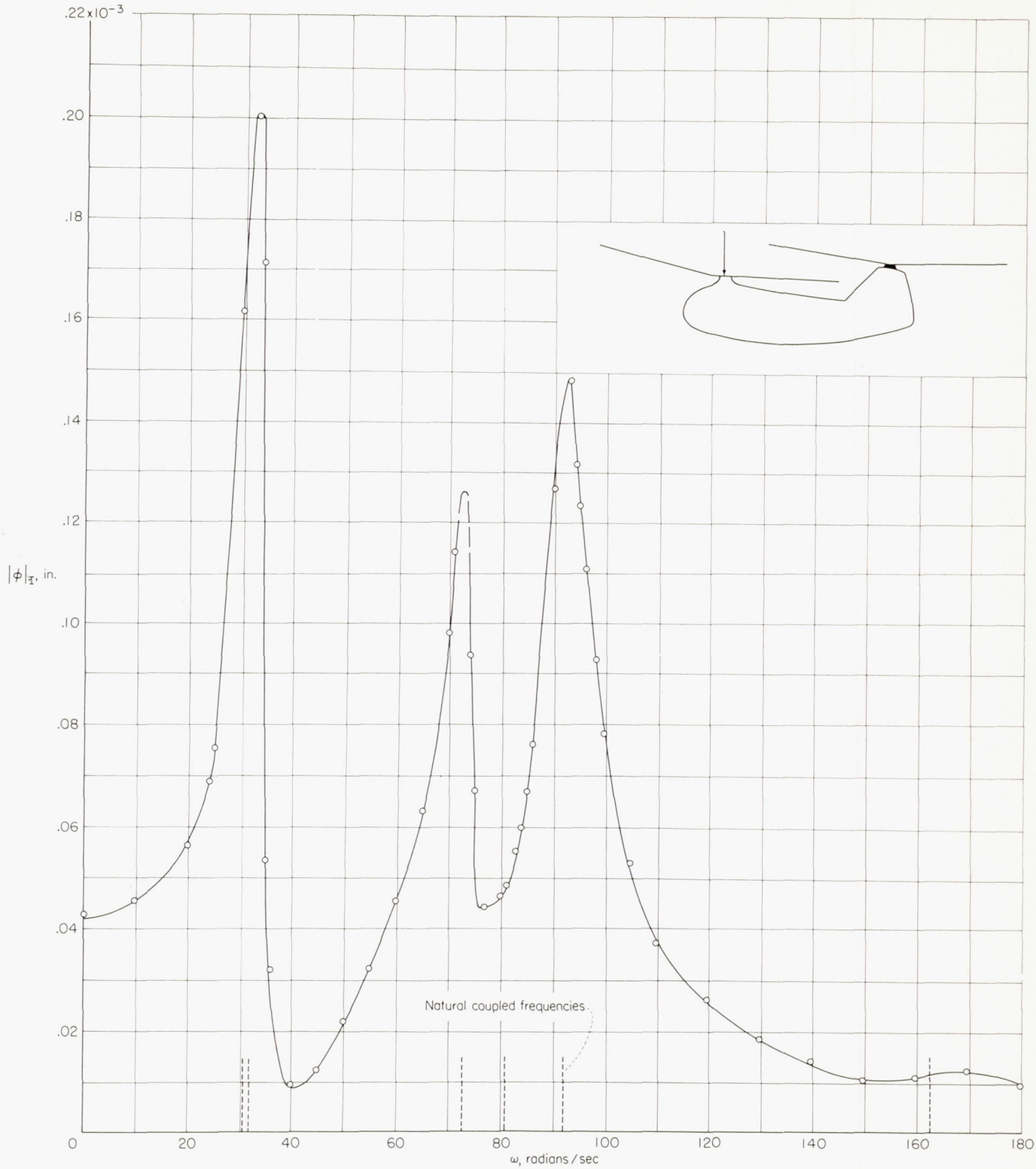

FIGURE II–9.—Effect of forcing frequency on amplitude of vibration of cockpit. Oscillating force of unit magnitude applied at front rotor hub.

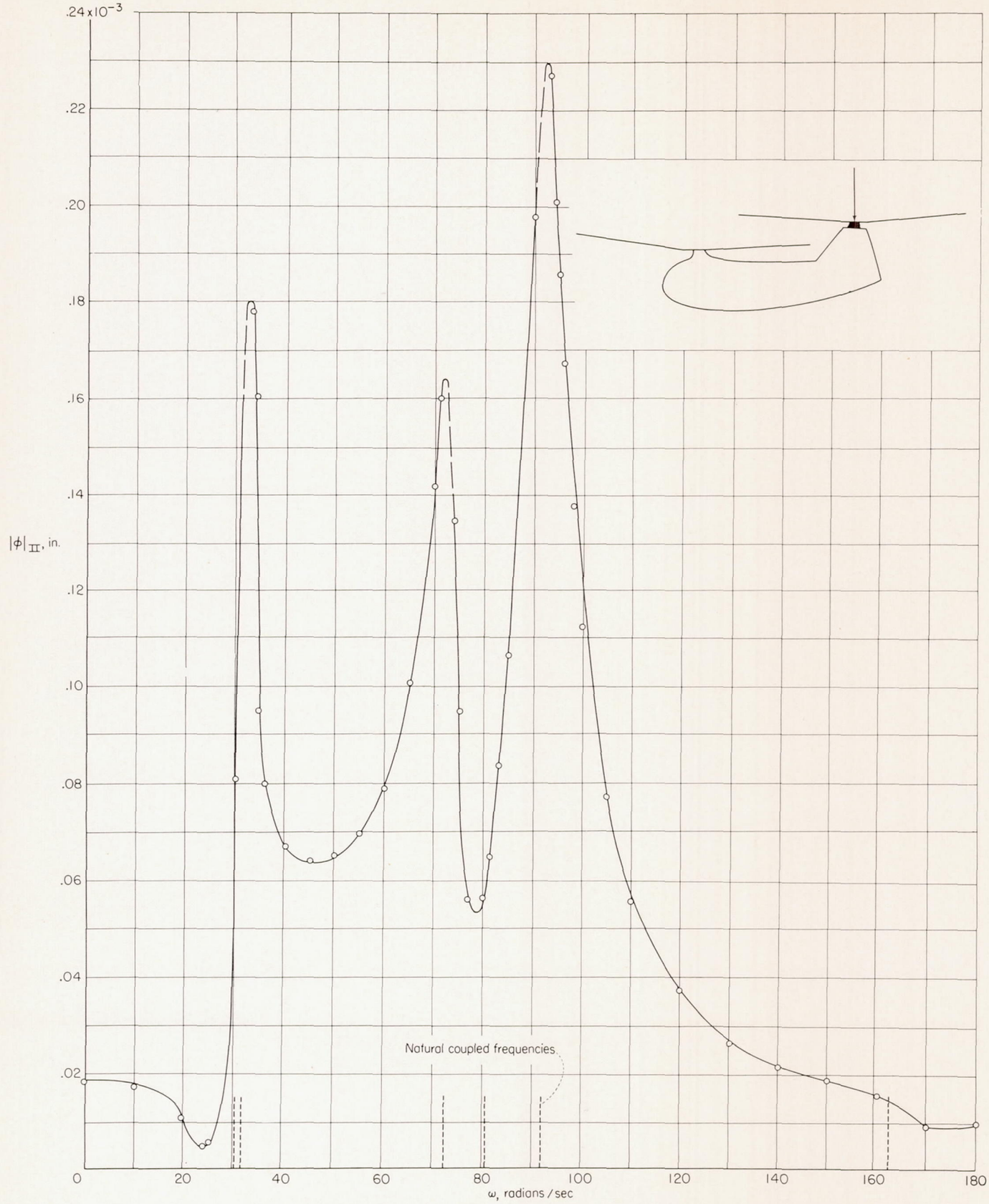

FIGURE II–10.—Effect of forcing frequency on amplitude of vibration of cockpit. Oscillating force of unit magnitude applied at rear rotor hub.

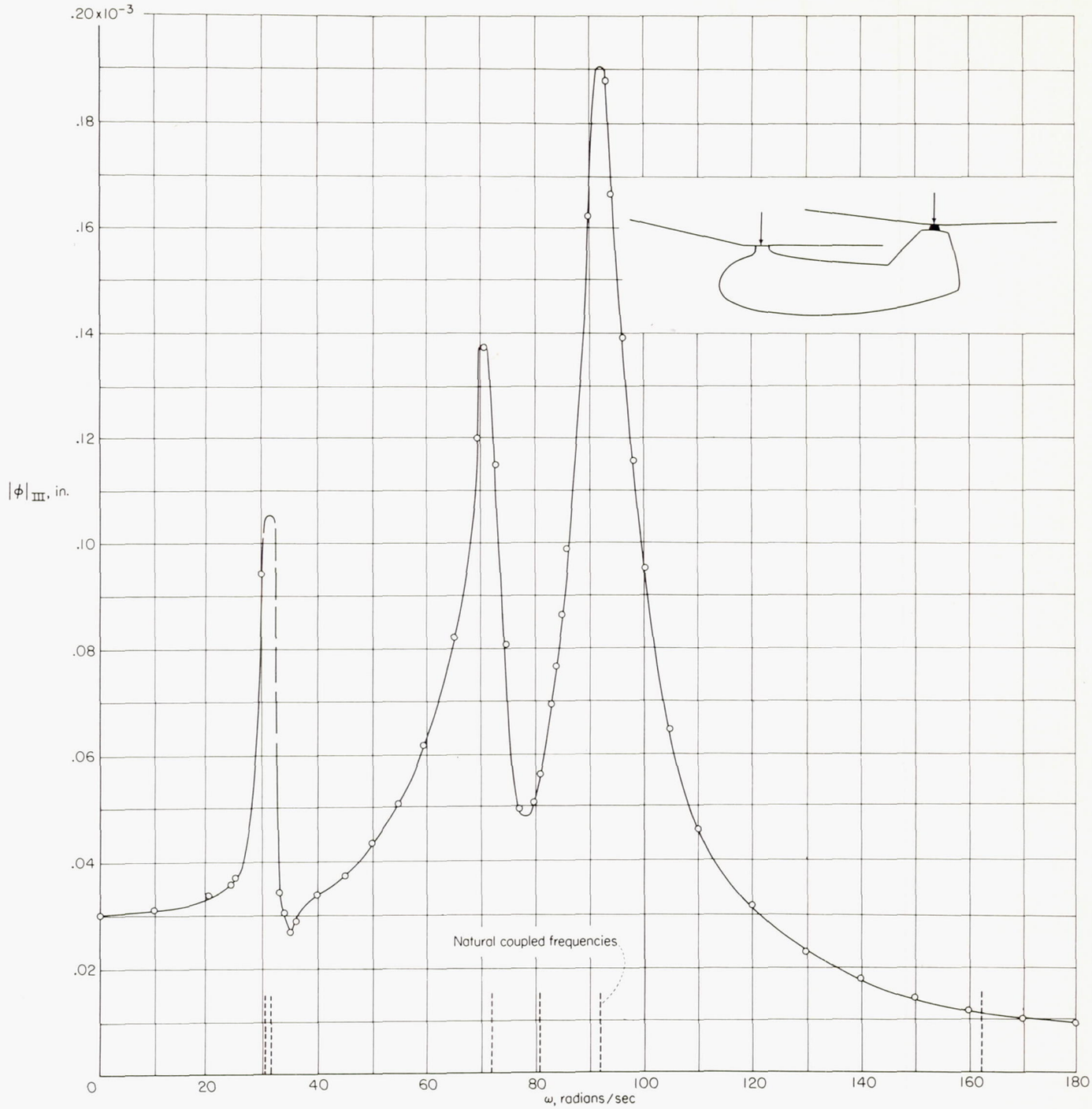

FIGURE II–11.—Effect of forcing frequency on amplitude of vibration of cockpit. Oscillating force of unit magnitude equally divided between front and rear rotor hubs and applied in same direction.

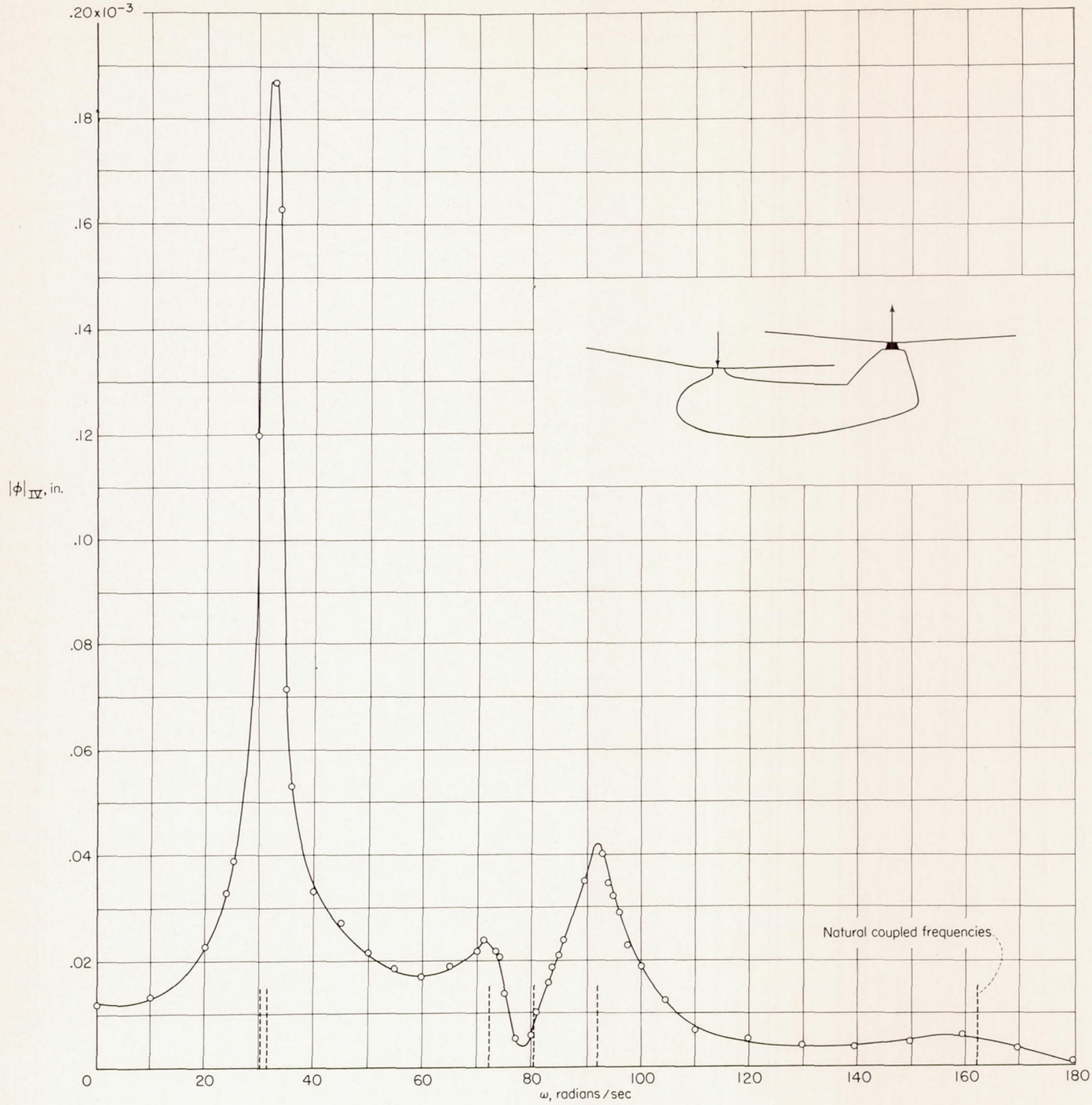

FIGURE II–12.—Effect of forcing frequency on amplitude of vibration of cockpit. Oscillating force of unit magnitude equally divided between front and rear rotor hubs and applied in opposite directions.

For one thing, the number of degrees of freedom treated, although they are believed to be the more important ones, are not nearly sufficient to predict all the coupled frequencies. A more complete analysis would also include the fore-and-aft motions of the front and rear rotor hubs, the pitching motions of the engine, and the chordwise motions of the blades in bending and rotation about the drag hinge. In fact, each blade should be treated as an independent flexible structure, subject only to the boundary conditions imposed by the vibrating hub to which it is attached. The complexities of treating such a system analytically are apparent and they exceed the intent of the present report.

The method of analysis presented in this report for the longitudinal vibrations—namely, the coupling of the structural properties of the uncoupled components of the helicopter to obtain the natural frequencies, mode shapes, and response of the coupled system—also appears applicable to the treatment of the case of coupled side bending and torsion of the fuselage. Vibrations of this type have been observed in tandem helicopters and a study of the effects of the significant parameters involved would provide useful design information.

CONCLUDING REMARKS

A method is presented for the calculation of the coupled frequencies and mode shapes of vibrations in the longitudinal plane of symmetry of tandem helicopters. The coupled frequencies and mode shapes are then used to calculate the response of the helicopter to applied loads. Sample calculations were made for an existing helicopter and these calculations yield the coupled frequencies and mode shapes and the deflection of the cockpit to oscillating loads applied at the front and rear rotor hubs. The mode shapes, both symmetrical and antisymmetrical, show the relative deflections of the various components of the structure when excited in a given mode.

The results of the calculations for the helicopter chosen show that the natural frequencies for the coupled modes may differ considerably from the natural frequencies for the uncoupled modes; therefore, there may be a need for making a rather comprehensive coupled-mode analysis so that regions of adverse dynamic response can be detected and avoided.

The results of calculations for different values of the uncoupled natural frequency of the fuselage indicate that the natural frequencies of the symmetrical coupled modes in the general range of the uncoupled frequency of the fuselage vary appreciably with changes in the uncoupled frequency of the fuselage; however, the effect on the natural frequency of the antisymmetrical coupled modes is negligible. An increase in the values of the Southwell coefficient for the blade first elastic flapwise bending mode resulted in a small increase in the coupled frequencies of both the antisymmetrical and symmetrical coupled modes having frequencies in the proximity of the blade frequencies.

The response calculations show that the amplitude of the vertical vibrations of the cockpit changes appreciably with changes in frequency, point of application, and manner of application of applied oscillating forces. High amplitudes occur when the frequencies of the applied oscillating forces are approximately equal to the natural frequencies of the second, third, and fifth coupled modes of the helicopter and the results of calculations indicate that the contributions of other modes to the vibrations of the cockpit are secondary for the specific forces chosen. The results indicate that the vibration of the cockpit due to oscillating forces having a frequency of 3 per revolution (3–P) or 90 radians per second are substantially greater for forces applied symmetrically at the front and rear rotor hubs than for forces applied antisymmetrically. The results also emphasize that it is very unlikely that all natural frequencies of a helicopter could be obtained by observing the response of the helicopter to oscillating forces applied at any given point.

APPENDIX

STEPS IN REDUCING THE ORDER OF THE MATRIX EQUATION

PROCEDURE WHEN $\Omega \neq 0$

When $\Omega \neq 0$, the matrix of the differential equations of motion, equation (11) of the text, can be written in concise notation of submatrices as follows:

$$[H]\{\eta\} = \begin{bmatrix} [\alpha] & [\beta] \\ [\beta]' & [\delta] \end{bmatrix} \begin{Bmatrix} \{\eta_1\} \\ \{\eta_2\} \end{Bmatrix} - \frac{1}{\omega^2} \begin{bmatrix} 0 & 0 \\ 0 & [\epsilon] \end{bmatrix} \begin{Bmatrix} \{\eta_1\} \\ \{\eta_2\} \end{Bmatrix} = 0 \tag{A1}$$

where

$$[\alpha] = \begin{bmatrix} M_f + M_e + pM_F + qM_R & M_e \frac{l_e}{l} + qM_R + M_f \frac{l_{cg}}{l} \\ M_e \frac{l_e}{l} + qM_R + M_f \frac{l_{cg}}{l} & M_f \left(\frac{k}{l}\right)^2 + M_e \left(\frac{l_e}{l}\right)^2 + qM_R \end{bmatrix} \tag{A2}$$

$$[\beta] = \begin{bmatrix} A_0 & B_0 & M_e y_1(l_e) + pM_F y_1(0) + qM_R y_1(l) & A_1 & B_1 & M_e \\ 0 & B_0 & M_e \frac{l_e}{l} y_1(l_e) + qM_R y_1(l) & 0 & B_1 & M_e \frac{l_e}{l} \end{bmatrix} \tag{A3}$$

$$[\beta]' = \text{Transpose of } [\beta] \tag{A4}$$

$$[\delta] = \begin{bmatrix} C_0 & 0 & y_1(0)A_0 & 0 & 0 & 0 \\ 0 & D_0 & y_1(l)B_0 & 0 & 0 & 0 \\ y_1(0)A_0 & y_1(l)B_0 & M_{f,1} + M_e y_1^2(l_e) + pM_F y_1^2(0) + qM_R y_1^2(l) & y_1(0)A_1 & y_1(l)B_1 & M_e y_1(l_e) \\ 0 & 0 & y_1(0)A_1 & C_1 & 0 & 0 \\ 0 & 0 & y_1(l)B_1 & 0 & D_1 & 0 \\ 0 & 0 & M_e y_1(l_e) & 0 & 0 & M_e \end{bmatrix} \tag{A5}$$

$$[\epsilon] = \begin{bmatrix} C_0\Omega^2 & & & & & \\ & D_0\Omega^2 & & & & \\ & & (\omega_{f,1})^2 M_{f,1} & & & \\ & & & C_1[(\omega_{F,1})^2 + K_{F,1}\Omega^2] & & \\ & & & & D_1[(\omega_{R,1})^2 + K_{R,1}\Omega^2] & \\ & & & & & M_e\omega_e{}^2 \end{bmatrix} \tag{A6}$$

$$\{\eta_1\} = \begin{Bmatrix} \tilde{b}_0 \\ \tilde{\tilde{b}}_0 \end{Bmatrix} \tag{A7}$$

and

$$\{\eta_2\}=\begin{Bmatrix}\tilde{a}_0\\ \tilde{c}_0\\ \tilde{b}_1\\ \tilde{a}_1\\ \tilde{c}_1\\ \tilde{w}_f\end{Bmatrix} \tag{A8}$$

If $[\alpha]\equiv\alpha$, $\{\eta_1\}\equiv\eta_1$, and so forth, then the algebraic expressions for the matrix equation, equation (A1), are as follows:

$$\alpha\eta_1+\beta\eta_2=0 \tag{A9}$$

$$\beta'\eta_1+\delta\eta_2=\frac{1}{\omega^2}\epsilon\eta_2 \tag{A10}$$

If equation (A9) is solved for η_1 and the result substituted into equation (A10), then

$$(\delta-\beta'\alpha^{-1}\beta)\eta_2=\frac{1}{\omega^2}\epsilon\eta_2 \tag{A11}$$

Multiplication of equation (A11) by the inverse of ϵ reduces it to the desired form; however, the resulting matrix is unsymmetrical and poorly conditioned. These characteristics are undesirable if iteration procedures are used to determine the frequencies and mode shapes, particularly so in this case because the frequencies are in some instances nearly equal to each other. The condition of the matrix can be improved and the matrix can be made symmetrical by the following transformation:

$$\sqrt{\epsilon}\,\eta_2=\xi \tag{A12}$$

which yields the final matrix

$$\left[\sqrt{\epsilon}^{-1}(\delta-\beta'\alpha^{-1}\beta)\sqrt{\epsilon}^{-1}-\frac{1}{\omega^2}\right]\xi=0 \tag{A13}$$

The natural frequencies are then obtained when the determinant of equation (A13) vanishes. When the natural frequencies are substituted back into the matrix (eq. (A13)) and the value of unity assigned to one of the coefficients (for example, ξ_η), the rest of the coefficients ξ_1, ξ_2, and so forth, can be obtained. If an iteration procedure is used, the values of ξ are determined simultaneously with the natural frequencies. In either case, the mode shapes are then obtained as follows:

$$\eta_1=-\alpha^{-1}\beta\sqrt{\epsilon}^{-1}\xi \tag{A14}$$

and

$$\eta_2=\sqrt{\epsilon}^{-1}\xi \tag{A15}$$

The relative magnitudes of the elements of equation (A13) are illustrated by the following matrix which results when $\Omega=30$ radians per second and the parameters are those for the basic configuration:

$$\begin{bmatrix}
0.0001715-\frac{1}{\omega^2} & -0.00002270 & 0.00008273 & -0.00001944 & 0.0001195 & -0.00002808\\
-0.00002270 & 0.00004242-\frac{1}{\omega^2} & -0.0000004435 & 0.0000001042 & -0.00003199 & 0.000007518\\
0.00008273 & -0.0000004435 & 0.001030-\frac{1}{\omega^2} & 0.00001907 & 0.00002841 & -0.000006676\\
-0.00001944 & 0.0000001042 & 0.00001907 & 0.0001563-\frac{1}{\omega^2} & -0.000006676 & 0.000001569\\
0.0001195 & -0.00003199 & 0.00002841 & -0.000006676 & 0.001039-\frac{1}{\omega^2} & 0.00001684\\
-0.00002808 & 0.000007518 & -0.000006676 & 0.000001569 & 0.00001684 & 0.0001568-\frac{1}{\omega^2}
\end{bmatrix}\begin{Bmatrix}\xi_1\\ \xi_2\\ \xi_3\\ \xi_4\\ \xi_5\\ \xi_6\end{Bmatrix}=0 \tag{A16}$$

PROCEDURE WHEN $\Omega=0$

When $\Omega=0$, the frequency parameter $1/\omega^2$ occurs in only the last four rows and columns of equation (11). The transformation of the matrix for the solution in this case is accomplished in the same fashion as for $\Omega\neq 0$ except that the submatrices (α, β, β', δ, ϵ, η_1, and η_2 of eq. (A1)) are of the fourth order. The relative magnitudes of the elements of the final matrix for $\Omega=0$ and for the basic parameters are shown by the following equation:

$$\begin{bmatrix} 0.0001516-\frac{1}{\omega^2} & -0.00006283 & -0.00009185 & -0.00001905 \\ -0.00006283 & 0.001515-\frac{1}{\omega^2} & 0.00001759 & -0.0000003405 \\ -0.00009185 & 0.00001759 & 0.001521-\frac{1}{\omega^2} & 0.00002506 \\ -0.00001905 & -0.0000003405 & 0.00002506 & 0.00004143-\frac{1}{\omega^2} \end{bmatrix} \begin{Bmatrix} \xi_1 \\ \xi_2 \\ \xi_3 \\ \xi_4 \end{Bmatrix} = 0 \tag{A17}$$

REFERENCES

1. Houbolt, John C., and Anderson, Roger A.: Calculation of Uncoupled Modes and Frequencies in Bending or Torsion of Nonuniform Beams. NACA TN 1522, 1948.
2. Myklestad, N. O.: Vibration Analysis. McGraw-Hill Book Co., Inc., 1944, pp. 184–214.
3. Brooks, George W.: Analytical Determination of the Natural Coupled Frequencies of Tandem Helicopters. Jour. Am. Helicopter Soc., vol. 1, no. 3, July 1956, pp. 39–52.
4. Yntema, Robert T.: Simplified Procedures and Charts for the Rapid Estimation of Bending Frequencies of Rotating Beams. NACA TN 3459, 1955. (Supersedes NACA RM L54G02.)

LANGLEY AERONAUTICAL LABORATORY,
NATIONAL ADVISORY COMMITTEE FOR AERONAUTICS,
LANGLEY FIELD, VA., *June 18, 1957.*

U. S. GOVERNMENT PRINTING OFFICE: 1958